

The advantages of the Eta model dynamics

Fedor Mesinger

fedor.mesinger@gmail.com

Serbian Academy of Sciences and Arts, Belgrade, Serbia

7th Workshop on the Eta model numerics,
characteristics, and applications

INPE, online, September 26, 2022

Eta dynamics: What is being done ?

- **Gravity-inertia wave terms**, B/E grid: forward-backward scheme that (1) avoids the time computational mode of the leapfrog scheme, and is **neutral with time steps twice leapfrog**;
(2) modified to enable propagation of a height point perturbation to its nearest-neighbor height points/ **suppress space computational mode**;
- **Split-explicit time differencing** (very efficient);
- Horizontal Arakawa advection that conserves **energy and C-grid enstrophy**, on the B/E grid, in space differencing (Janjić 1984);
- Conservation of **energy in transformations between the kinetic and potential energy**, in space differencing;
- **Finite-volume vertical advection** of dynamic variables (v, T)
- **Nonhydrostatic option**;
- The **(cut-cell) eta vertical coordinate**, ensuring hydrostatically consistent calculation of the pressure gradient (“second”) term of the pressure-gradient force (PGF);

Before we get into some of these:

To solve our equations we use **values at grid points**:

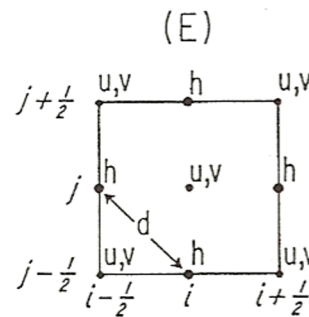
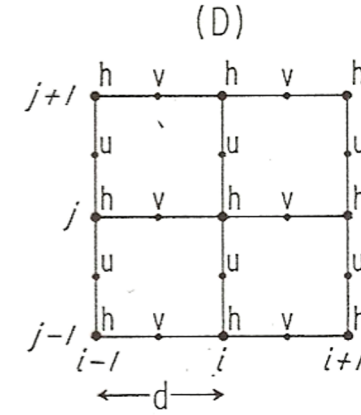
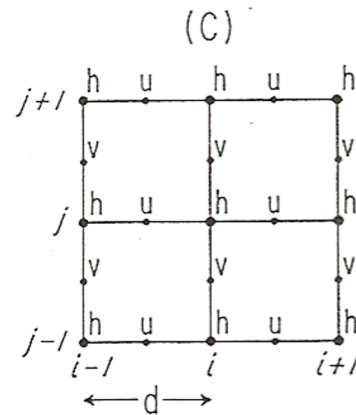
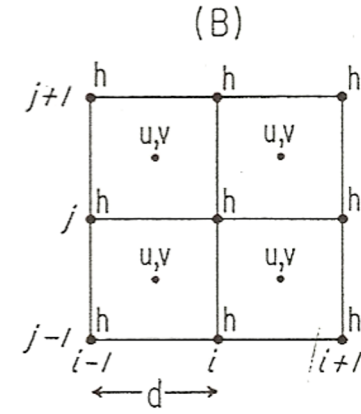
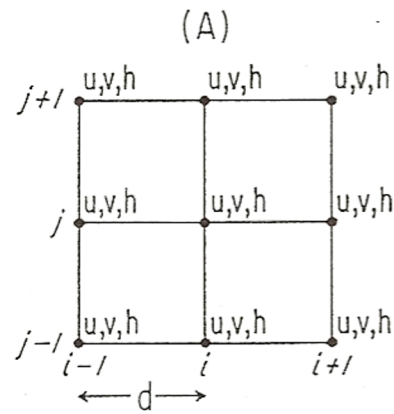
we need a horizontal grid, and a vertical grid

horizontal

Primitive equations

Four possible square grids:

Note:
E grid is same as B but rotated 45°. Thus, often: E/B, or B/E

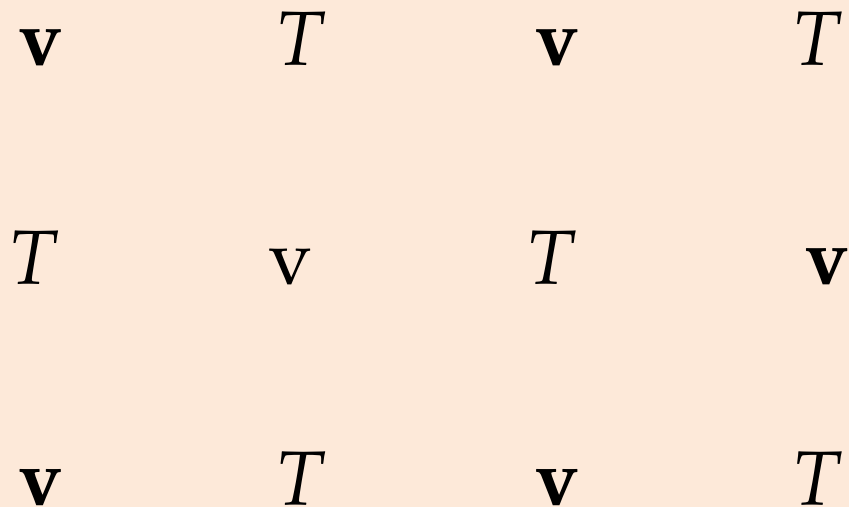


The Eta

FIG. 3. Spatial distributions of the dependent variables on a square grid.

What are the **values at the grid points** ?

With “primitive equations”, and the E grid horizontal grid consists of $\mathbf{v}(u,v)$, and T points:



Two main possibilities: **values of continuous fields**, taken at points, or **averages over grid cells**

Averages over grid cells:

Reynolds averages

This view taken in the Eta dynamics,

“Finite-volume” approach

With this approach formal, Taylor series type order of accuracy, has a questionable meaning

In slide #2, **eight** features have been listed. Their purposes are different

- Some, to increase accuracy by avoiding recognized possible errors,
- Others, same, but by avoiding “computational modes”,
- Still others, same, but by maintaining integral properties,
- Yet others, to increase computational efficiency, along with some of the above

Eta dynamics: What is being done ?

- **Gravity-inertia wave terms**, B/E grid: forward-backward scheme that (1) avoids the time computational mode of the leapfrog scheme, and is **neutral with time steps twice leapfrog**;
(2) modified to enable propagation of a height point perturbation to its nearest-neighbor height points/ **suppress space computational mode**;
- **Split-explicit time differencing** (very efficient);
- Horizontal Arakawa advection that conserves **energy and C-grid enstrophy**, on the B/E grid, in space differencing (Janjić 1984);
- Conservation of **energy in transformations between the kinetic and potential energy**, in space differencing;
- **Finite-volume vertical advection** of dynamic variables (v, T)
- **Nonhydrostatic option**;
- The **(cut-cell) eta vertical coordinate**, ensuring hydrostatically consistent calculation of the pressure gradient (“second”) term of the pressure-gradient force (PGF);

Eta dynamics: What is being done ?

- Gravity wave terms, on the B/E grid: forward-backward scheme that (1) avoids the time computational mode of the leapfrog scheme, and is neutral w.r.t. the spurious energy; (2) modified to enable propagation of a height point perturbation to its nearest-neighbor height point; computational mode;
- Split-explicit time differencing (very efficient);
- Horizontal Arakawa advection that conserves **energy and C-grid enstrophy**, on the B/E grid, in space differencing (Janjić 1984);
- Conservation of energy in transformations between the kinetic and potential energy, in space differencing;
- **Finite-volume vertical advection of dynamic variables (v, T)**
- Nonhydrostatic option;
- The **(cut-cell) eta vertical coordinate**, ensuring hydrostatically consistent calculation of the pressure gradient (“second”) term of the pressure-gradient force (PGF);

Arakawa horizontal advection schemes

The first “general circulation” experiment:

Phillips, N. A., 1956. *The general circulation of the atmosphere: a numerical experiment*. Quart. J. Roy. Meteor. Soc., 82, 123-164.

A problem: features / energy was accumulating at small scales

Arakawa energy / enstrophy conserving schemes address

Nondivergent
vorticity
equation,
Arakawa
(1966):

$$\frac{\partial \zeta}{\partial t} + \mathbf{v} \cdot \nabla \zeta = 0; \quad \zeta = \nabla^2 \psi, \quad (7.1)$$

where the velocity \mathbf{v} is assumed to be nondivergent, that is

$$\mathbf{v} = \mathbf{k} \times \nabla \psi. \quad (7.2)$$

Substituting this into (7.1) we obtain

$$\frac{\partial}{\partial t} \nabla^2 \psi = J(\nabla^2 \psi, \psi). \quad (7.3)$$

$$\psi = \sum_n \psi_n, \text{ (e.g. Courant and Hilbert, 1953, p. 369)} \quad (7.4)$$

where the functions ψ_n are eigenfunctions of the Helmholtz equation

$$\nabla^2 \psi_n + \lambda_n^2 \psi_n = 0. \quad (7.5)$$

The parameters λ_n are known as the generalized wavenumbers of the components ψ_n .

As an example, let A be a rectangular region with sides L_x, L_y . For boundary conditions assume that the stream function is periodic in A : with period L_x and is zero along the lower and upper boundary. Then we can write the stream function

$$\psi = \sum_{n_1, n_2} \left(a_{n_1 n_2} \cos \frac{2\pi n_1}{L_x} x + b_{n_1 n_2} \sin \frac{2\pi n_1}{L_x} x \right) \sin \frac{\pi n_2}{L_y} y. \quad (7.6)$$

Differentiating this we obtain

$$\nabla^2 \psi_n = - \left[\left(\frac{2\pi n_1}{L_x} \right)^2 + \left(\frac{\pi n_2}{L_y} \right)^2 \right] \psi_n, \quad \lambda_n^2 = \left(\frac{2\pi n_1}{L_x} \right)^2 + \left(\frac{\pi n_2}{L_y} \right)^2$$

$$\bar{K} = -\frac{1}{2} \sum_m \sum_n \overline{\psi_m \nabla^2 \psi_n} = \frac{1}{2} \sum_m \sum_n \lambda_n^2 \overline{\psi_m \psi_n}$$

Since the functions ψ_n are orthogonal, that is,

$$\overline{\psi_m \psi_n} = 0 \text{ for } m \neq n,$$

We have therefore expressed the average kinetic energy in the region A *as a sum of contributions of different harmonics*

$$\bar{K} = \sum_n K_n, \quad (7.8)$$

where
$$K_n \equiv \frac{1}{2} \lambda_n^2 \overline{\psi_n^2}.$$

Very similar for the mean square vorticity:

$$\overline{\zeta^2} = \overline{(\nabla^2 \psi)^2}$$

can be expressed as a sum of contributions of different harmonics in a similar way. Substituting (7.4), using (7.5), and the orthogonality of the functions ψ_n , we obtain

$$\overline{\zeta^2} = \sum_n \lambda_n^4 \overline{\psi_n^2}. \quad (7.10)$$

$$\psi = \sum_n \psi_n \quad (7.4)$$

$$\nabla^2 \psi_n + \lambda_n^2 \psi_n = 0 \quad (7.5)$$

Substituting the expression (7.9) for the kinetic energy of a component ψ_n ; we find for the average value of the enstrophy, half the vorticity squared,

$$K_n \equiv \frac{1}{2} \lambda_n^2 \overline{\psi_n^2}. \quad (7.9)$$

$$\frac{1}{2} \overline{\zeta^2} = \sum_n \lambda_n^2 K_n. \quad (7.11)$$

Comparing this with (7.8) we see that the average wavenumber is related to average values of enstrophy and kinetic energy. Define the average wavenumber as

$$\lambda \equiv \sqrt{\frac{\sum_n \lambda_n^2 K_n}{\sum_n K_n}}. \quad (7.12)$$

Substituting (7.11) and (7.8) we find

$$\lambda = \sqrt{\frac{1}{2} \frac{\overline{\zeta^2}}{\overline{K}}}. \quad (7.13)$$

Thus: when the velocity is two-dimensional and nondivergent, **the average wavenumber is determined by the ratio of the average values of enstrophy and kinetic energy !**

From (7.13) and (7.11):

$$\bar{K}\lambda^2 = \frac{1}{2}\overline{\zeta^2} = \sum_n \lambda_n^2 K_n = \text{const} \quad \text{as pointed out by Charney (1966):}$$

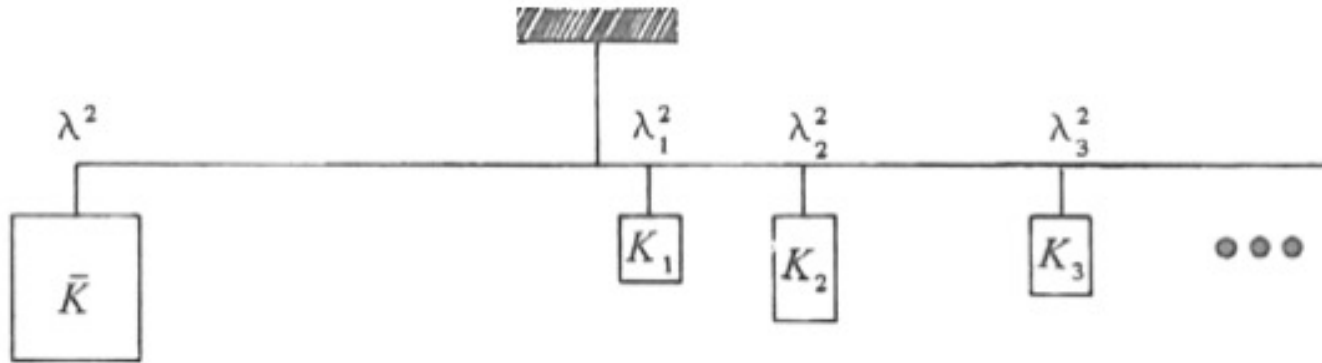


Figure 7.1 A mechanical analogy of the interchange of energy between harmonic components

From (7.13) and (7.11):

$$\bar{K}\lambda^2 = \frac{1}{2}\overline{\zeta^2} = \sum_n \lambda_n^2 K_n = \text{const} \quad \text{as pointed out by Charney (1966):}$$

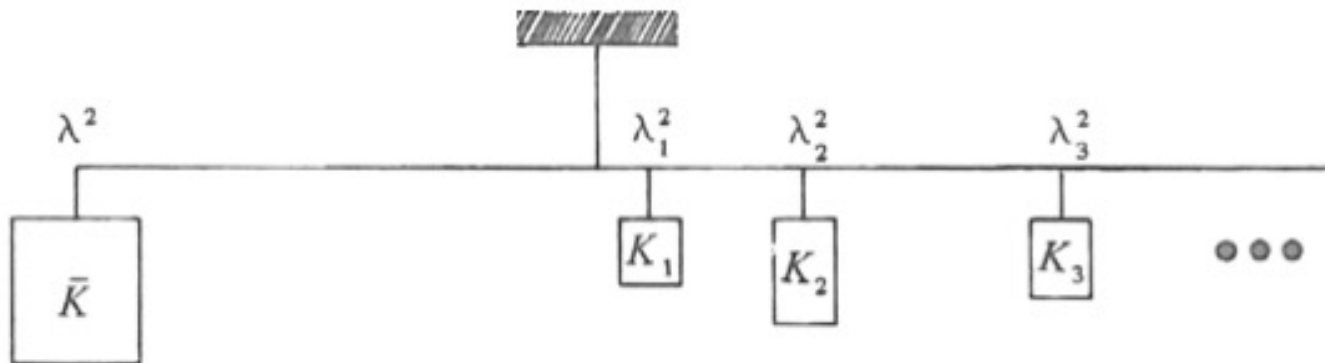
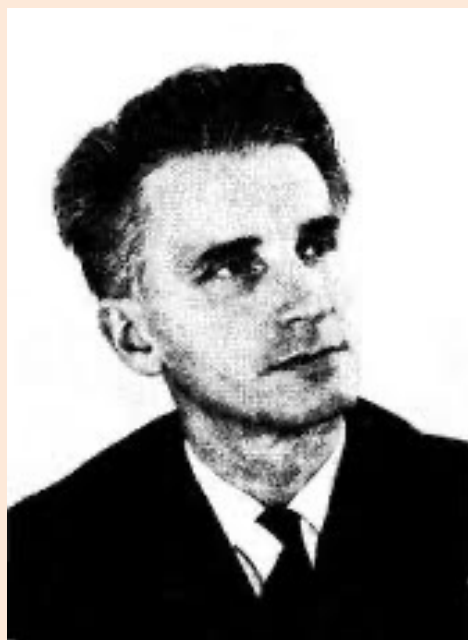


Figure 7.1 A mechanical analogy of the interchange of energy between harmonic components

Ragnar
Fjørtoft
(1913-1998)



From (7.13) and (7.11):

$$\bar{K}\lambda^2 = \frac{1}{2}\overline{\zeta^2} = \sum_n \lambda_n^2 K_n = \text{const} \quad \text{as pointed out by Charney (1966):}$$

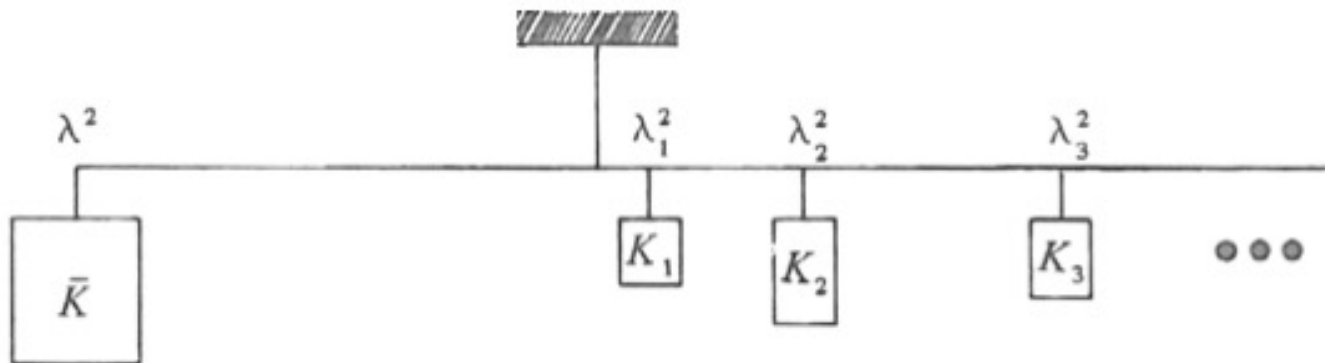
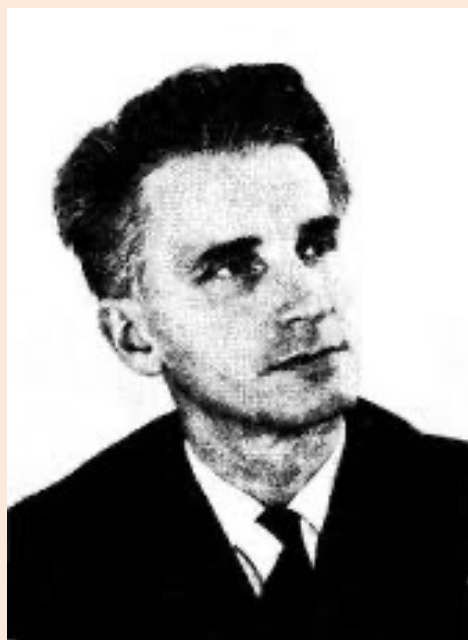


Figure 7.1 A mechanical analogy of the interchange of energy between harmonic components

Ragnar
Fjørtoft
(1913-1998)



Jule
Charney
(1917-1981)



Early NWP and general circulation (Norman Phillips !)
experience has shown that numerical models have problems
in behaving quite differently - energy accumulating at small
scales, with catastrophic results :(

Can one reproduce this feature of the continuous
equations ?

Akio Arakawa ! (1966)

International symposium on numerical weather
forecasting Oslo, March 11-16, 1963

We illustrate Arakawa's method by considering how to satisfy (7.17)₁. In our finite difference calculation it takes the form

$$\overline{\zeta_{ij} J_{ij}(\zeta, \psi)} = \frac{1}{N} \sum_{i,j} \zeta_{ij} J_{ij}(\zeta, \psi) = 0, \quad (7.19)$$

(7.17)₁:

$$\overline{pJ(p,q)} = 0$$

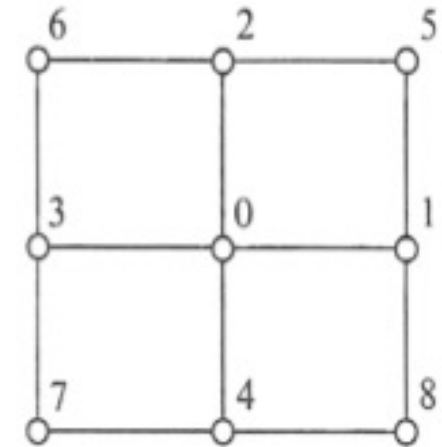
$$\begin{aligned} J(p,q) &= \frac{\partial p}{\partial x} \frac{\partial q}{\partial y} - \frac{\partial p}{\partial y} \frac{\partial q}{\partial x} = \frac{\partial}{\partial y} \left(q \frac{\partial p}{\partial x} \right) - \frac{\partial}{\partial x} \left(q \frac{\partial p}{\partial y} \right) = \\ &= \frac{\partial}{\partial x} \left(p \frac{\partial q}{\partial y} \right) - \frac{\partial}{\partial y} \left(p \frac{\partial q}{\partial x} \right). \end{aligned}$$

$$J^{++}(p,q) = \frac{1}{4d^2} \left[(p_1 - p_3)(q_2 - q_4) - (p_2 - p_4)(q_1 - q_3) \right], \quad (7.21a)$$

$$\begin{aligned} J^{\times+}(p,q) &= \frac{1}{4d^2} \left[q_2(p_5 - p_6) - q_4(p_8 - p_7) \right. \\ &\quad \left. - q_1(p_5 - p_8) + q_3(p_6 - p_7) \right], \end{aligned} \quad (7.21b)$$

$$\begin{aligned} J^{+\times}(p,q) &= \frac{1}{4d^2} \left[p_1(q_5 - q_8) - p_3(q_6 - q_7) \right. \\ &\quad \left. - p_2(q_5 - q_6) + p_4(q_8 - q_7) \right]. \end{aligned} \quad (7.21c)$$

More general: $J(p,q) = \alpha J^{++} + \beta J^{\times+} + \gamma J^{+\times} \quad (7.22)$



not only do all the terms in the sum (7.19) cancel, but also all the terms in the expression for the conservation of the average kinetic energy, and the average vorticity (Arakawa, 1966; Lilly, 1965). Thus, the approximation

$$J_A \equiv \frac{1}{3} (J^{++} + J^{\times+} + J^{+\times}), \quad (7.23)$$

will conserve average vorticity, enstrophy and kinetic energy when used for the numerical solution of (7.3). This is more than sufficient for the prevention of non-linear instability. The approximation (7.23) is usually called the *Arakawa Jacobian*. Arakawa has also shown how to construct an approximation of fourth order accuracy to the Jacobian, conserving these three quantities.

Arakawa vorticity equation scheme transformed to the C-grid:

Arakawa A. and V. R. Lamb, 1977: Computational design of the basic dynamical processes of the UCLA general circulation model. *Methods in Computational Physics*, J. Chang, Ed., Academic Press, 174–264. (“The Green Book”)

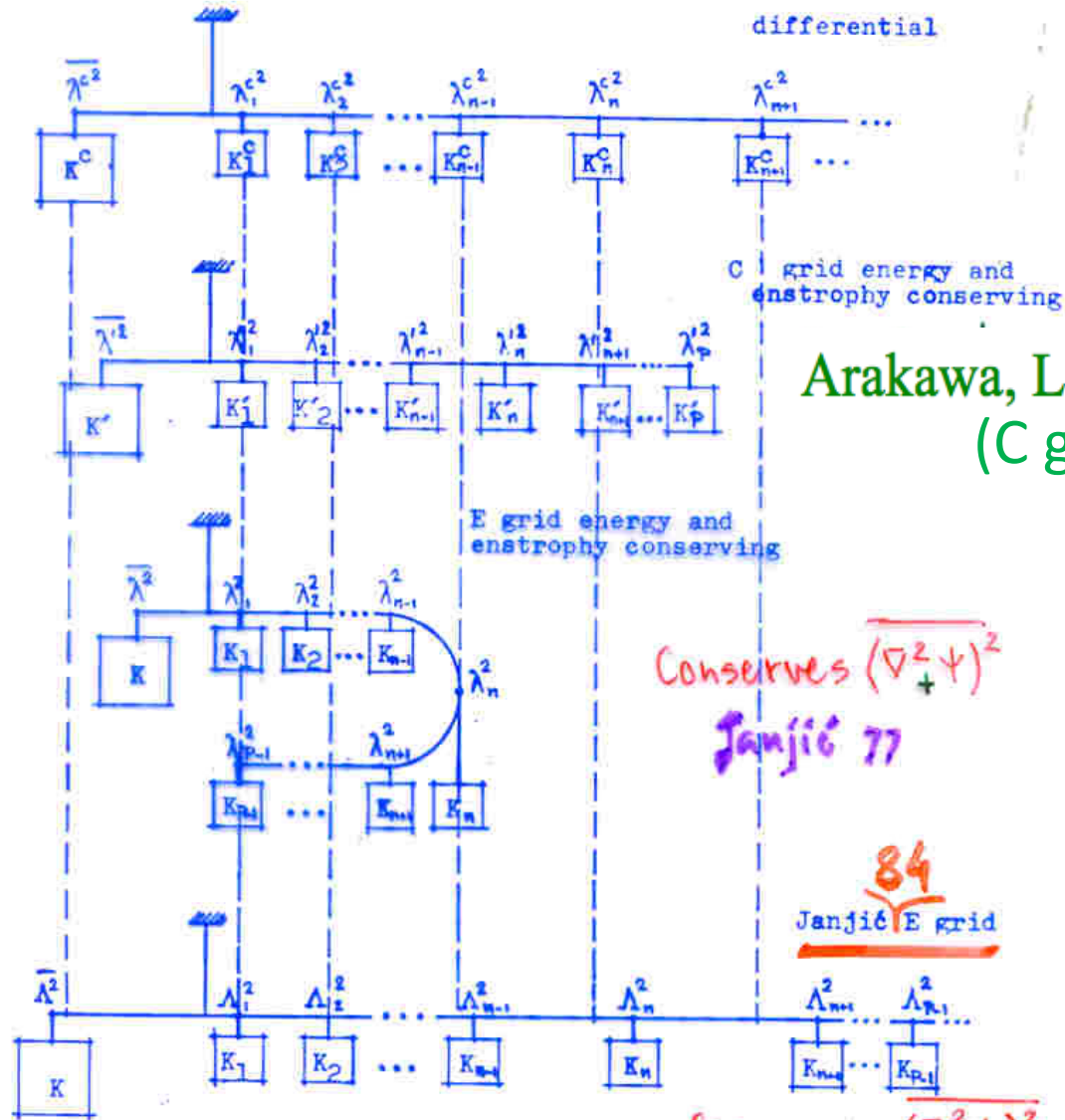
The C-grid Arakawa scheme transformed to the B/E-grid:

Janjić, Z. I., 1984: Nonlinear advection schemes and energy cascade on semi-staggered grids. *Mon. Wea. Rev.*, **112**, 1234-1245.

From ECMWF Seminar 1983:

The horizontal advection scheme:

Nondivergent, barotropic flow;



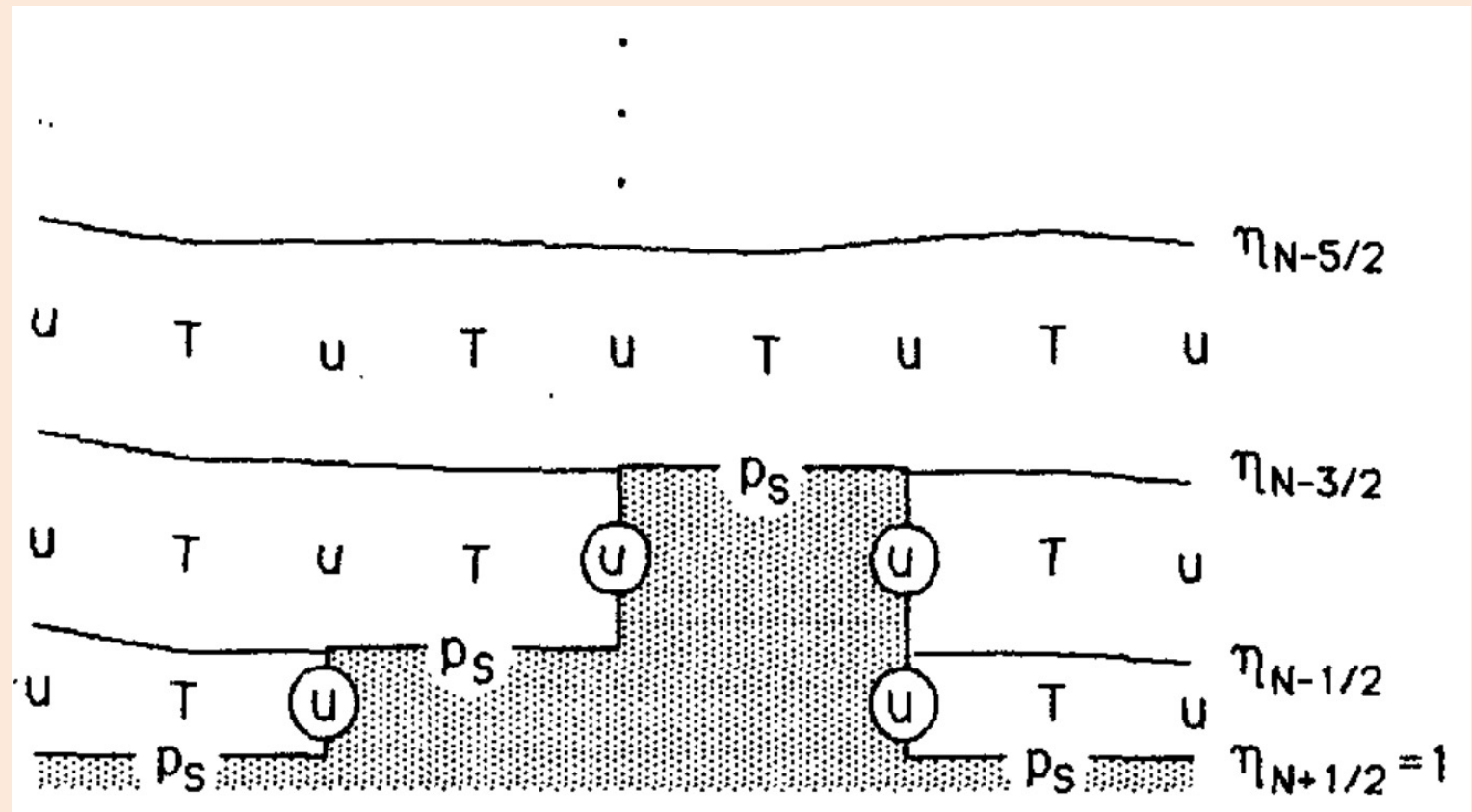
Arakawa, Lamb (1977)
(C grid)

(B/E grid)
Janjić 1984

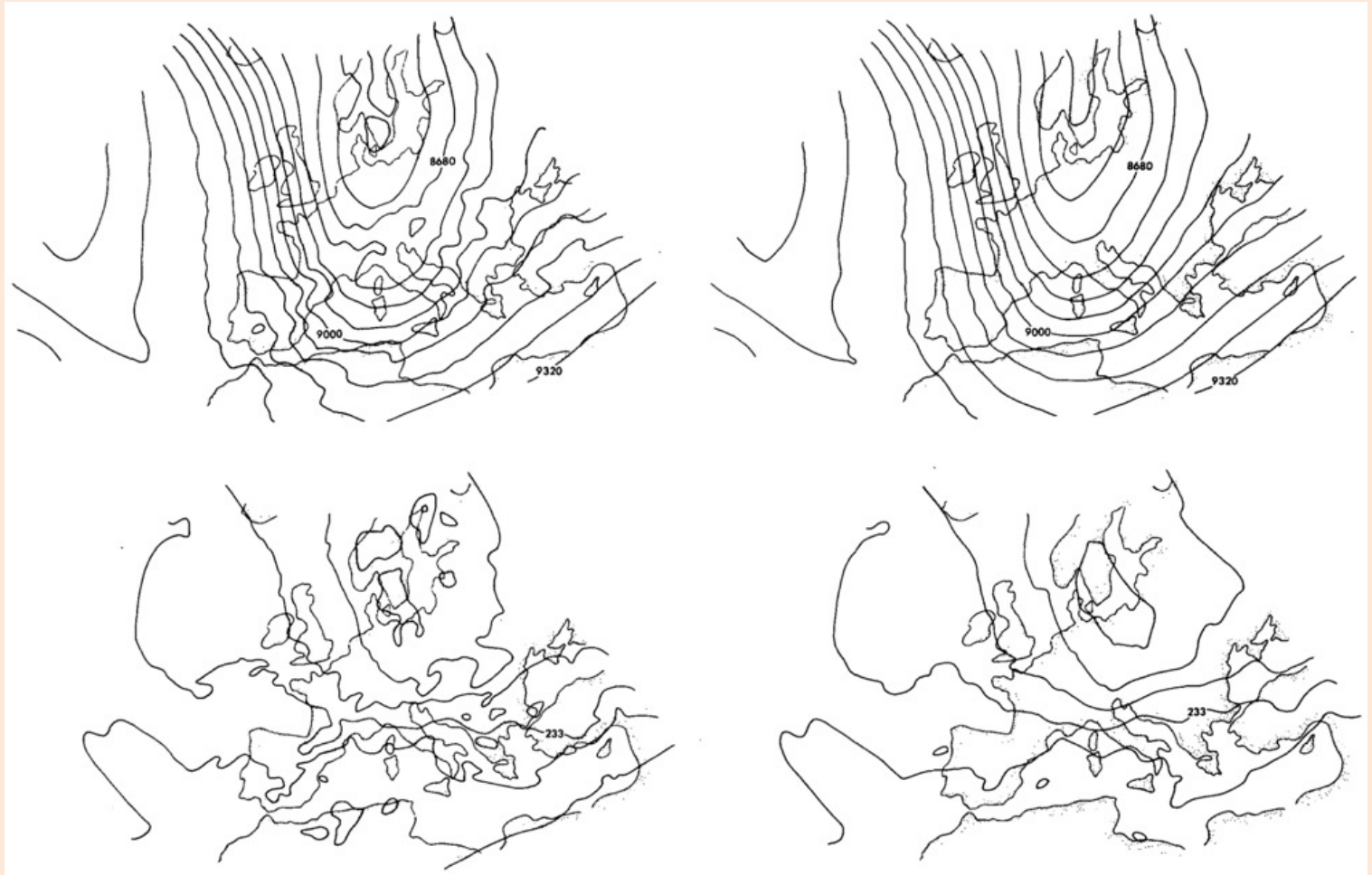
Fig. 3.12. Mechanical analogies of the constraints imposed on the non-linear energy cascade in the continuous case, in the case of the C-grid energy and enstrophy conserving scheme, in the case of the E-grid energy and enstrophy conserving scheme, and in the case of the scheme due to Janjić (1984).

96 (ECMWF Seminar '83)

->
The
Eta
model



300 hPa
geopotential
heights (above)
and temperatures
(below) in a 48-h
simulation using
the sigma system
(left) and using
the eta system
(right). Contour
intervals are 80 m
for geopotential
heights, and 2.5 K
for temperature.
From Mesinger et
al. (1988)



Eta primary regional operational model at U.S. National Meteorological Center as of **March 1993**. At INPE, **1996**..

....

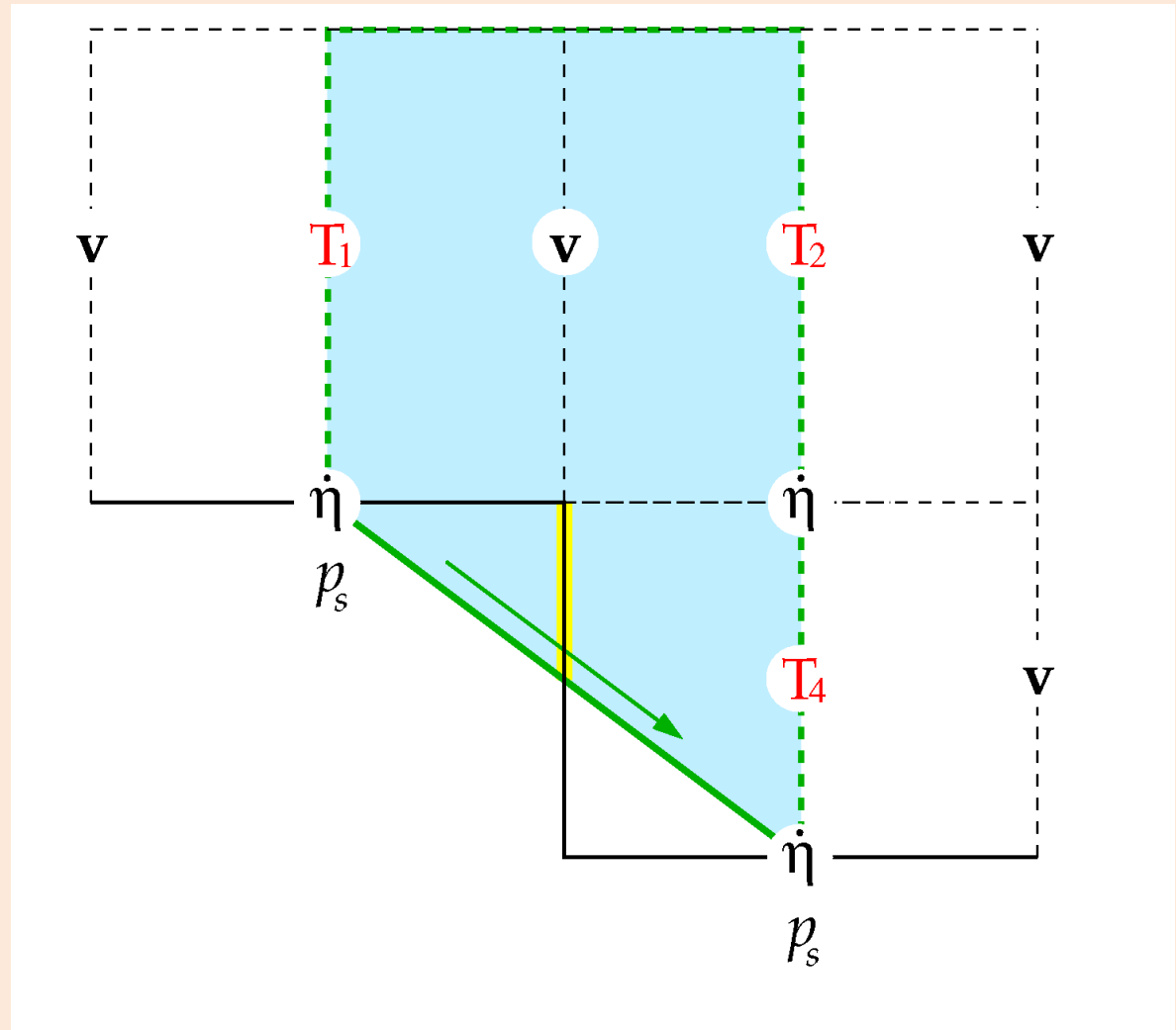
However,

- Experimental 10-km Eta did poorly a windstorm in the lee of Wasatch mountain, while a sigma system MM5 did well,
- Gallus and Klemp (2000) published experiments on flow over a bell-shaped topography. Gallus and Rančić eta coordinate model failed to simulate downstream flow, instead had the flow in the lee separate off the top of the topography

Gallus and Klemp ascribed the problem to the existence of step corners of the step topography Eta, therefore:

The sloping steps (a simple **cut-cell scheme**), vertical grid:

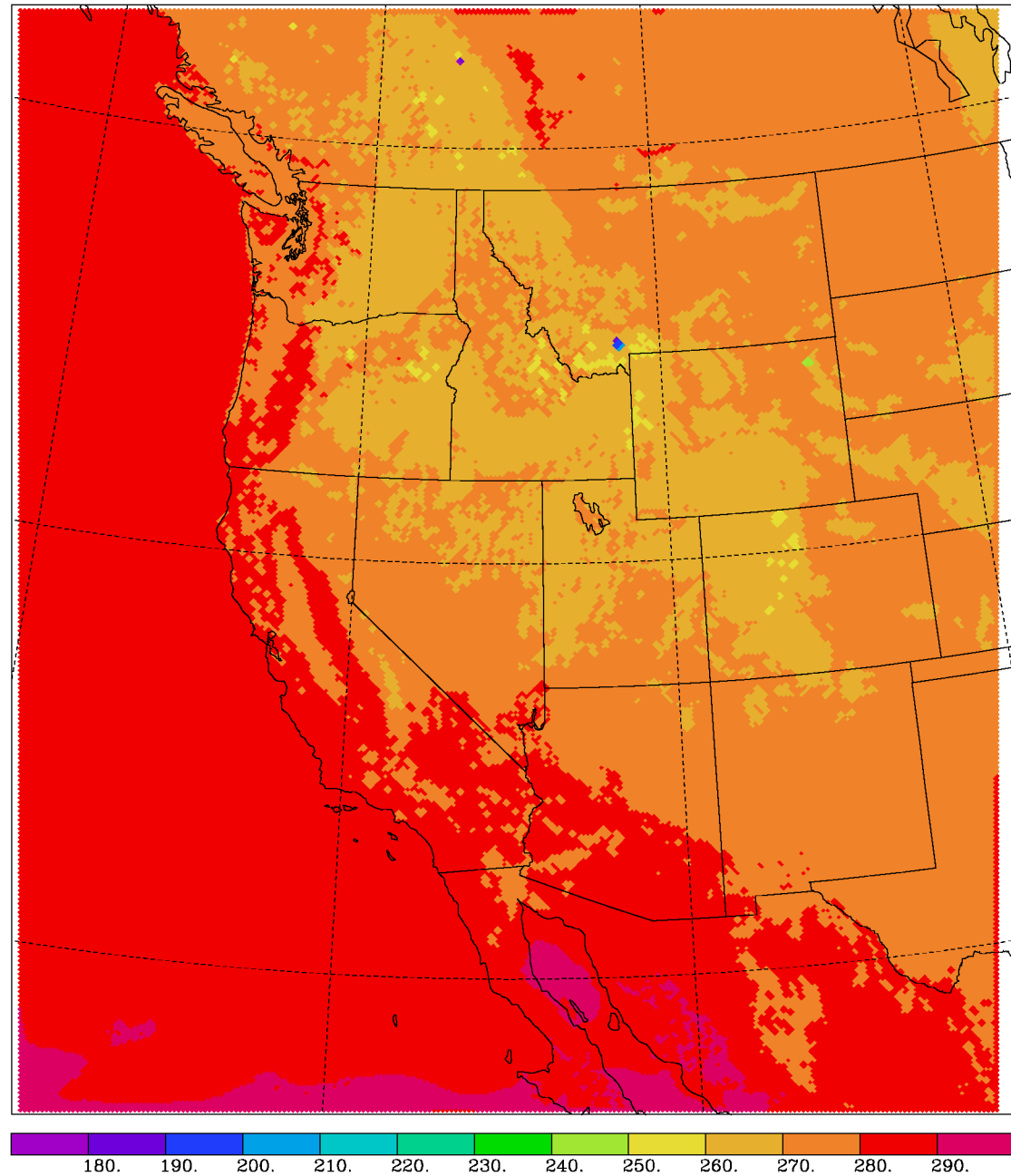
The central **v** box exchanges momentum, on its right side, with **v** boxes of **two** layers, and **T_1** box undergoes horizontal advection to **T_2** and vertical (slantwise) advection to **T_4**

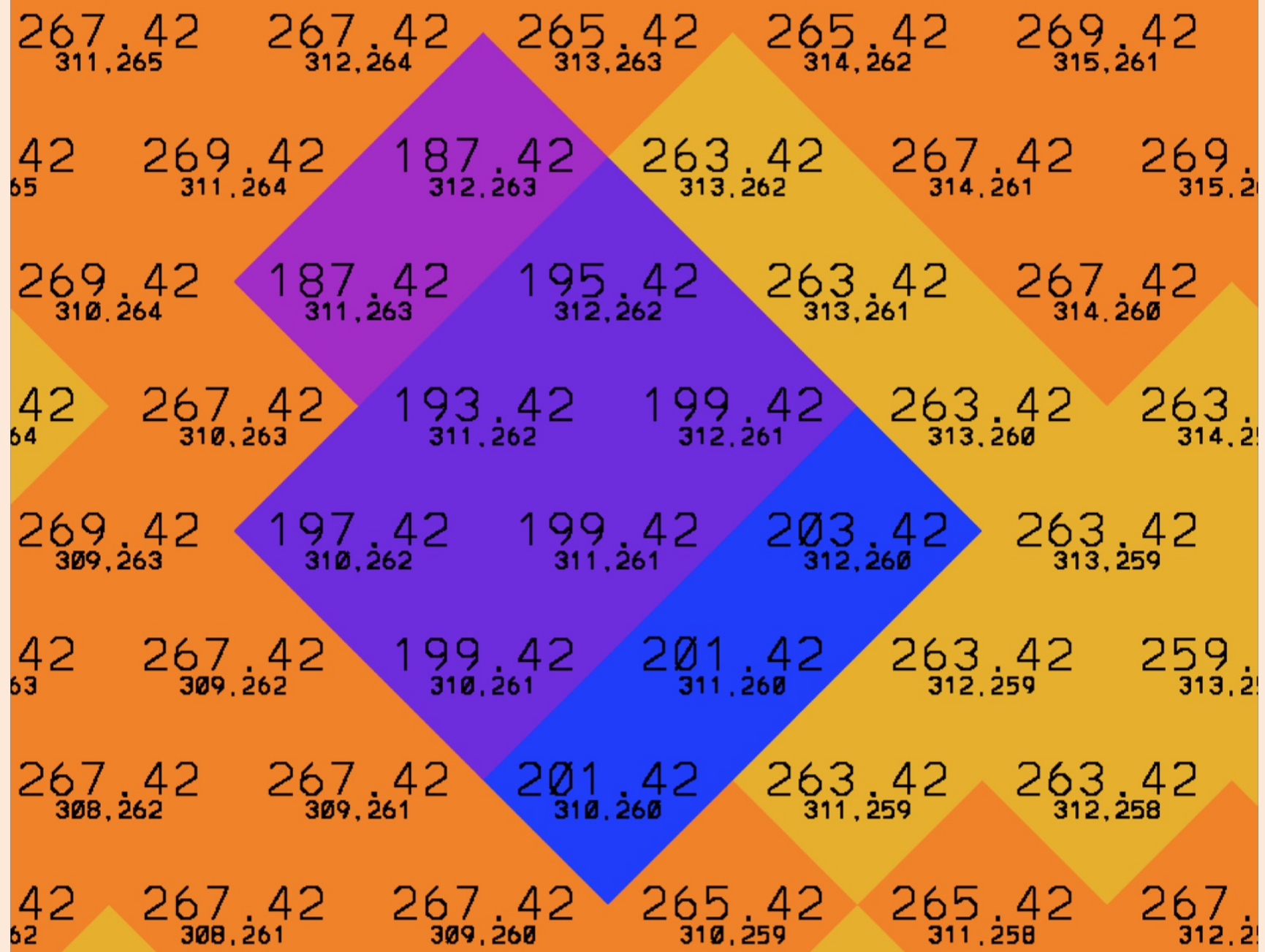


When this
was coded
and tested,
48-h lowest T
boxes map:

VALID 11 Dec 2005 12Z Sunday

20051209 12UTC 48h fcst





Suspect: slantwise T advection:

standard “Lorenz-Arakawa” centered vertical advection scheme (Arakawa and Lamb 1977)

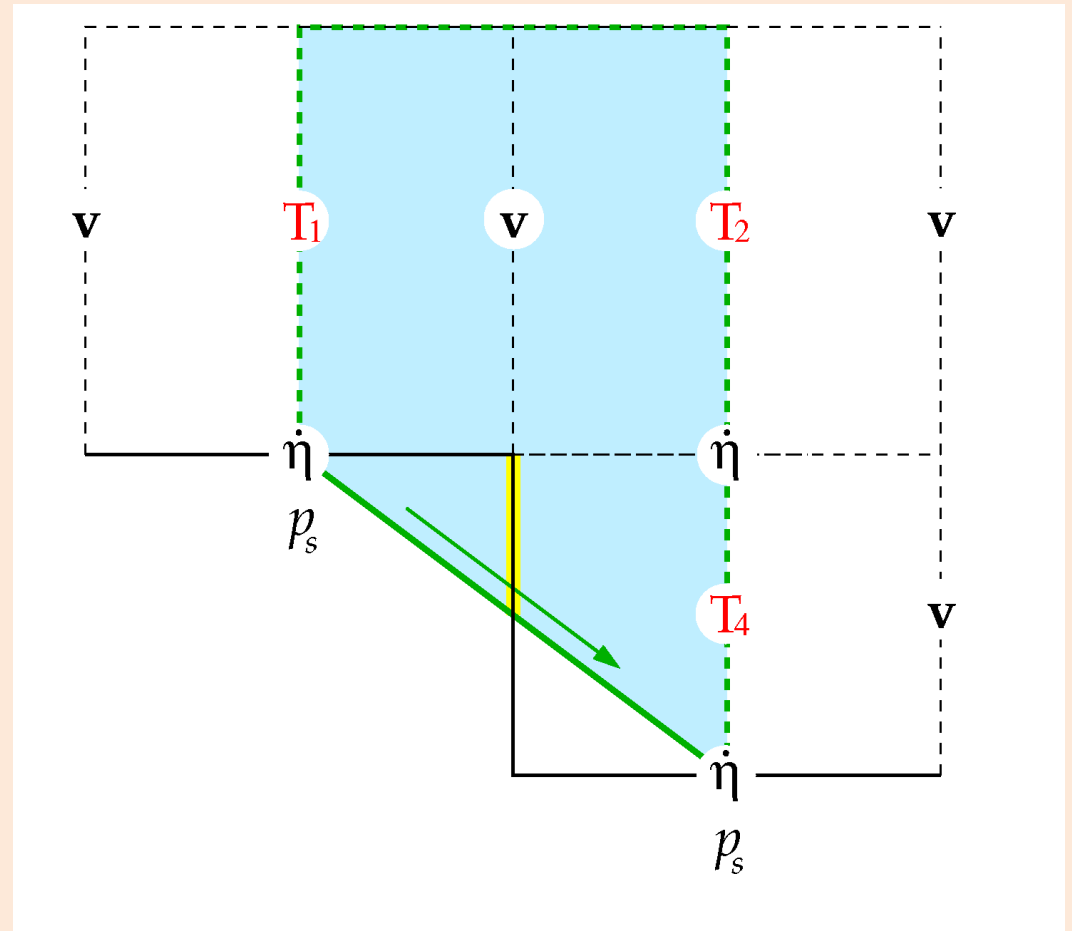
$$\frac{\partial T}{\partial t} = \dots - \dot{\eta} \overline{\frac{\partial T}{\partial \eta}} \quad (2)$$

It allows a false vertical advection from below ground !!

If a temperature inversion were to develop at the bottom of a basin, with a persistent upward motion, then the vertical advection contribution from the interface between the lowest T cell and the one above it would cool both cells, but for the lower of them would be the only contribution, thus tending to increase the inversion, amplifying its cooling, feeding on itself !!!

In addition, this advection into the lowest cell, is **physically wrong**,
no advection should exist
into the lowest cell
from below ground !!

But with the finite-volume
approach, with \mathbf{v} constant
inside the bluish \mathbf{v} cell, as
well as the T_1 and T_4 inside
their cells, **we can calculate**
how much air is crossing the
yellow line **and replace the**
wrong slantwise advection
with correct T changes !!!

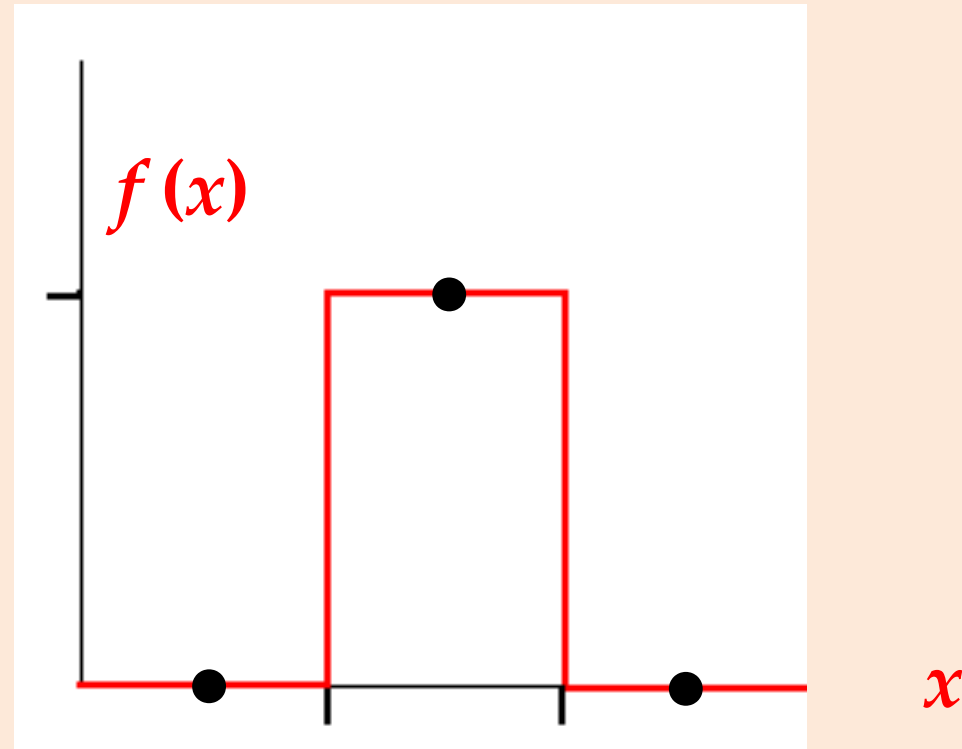


Done, however

Since the problem exists in vertical advection as well, vertical advection of v and T replaced as well !!

Piecewise linear (finite-volume) advection scheme used

Consider advection of a top hat (or step) function, e.g.:



Creation of false maxima or minima using centered schemes !

Advection of moisture :(

From Mesinger, Jovic (NCEP Office Note 2002):

Slope adjustment scheme

Slopes can be adjusted, but no new maxima or minima must be created. This is the first iteration. If we are not next to a minimum or maximum, we can go only half of the smaller of two sides

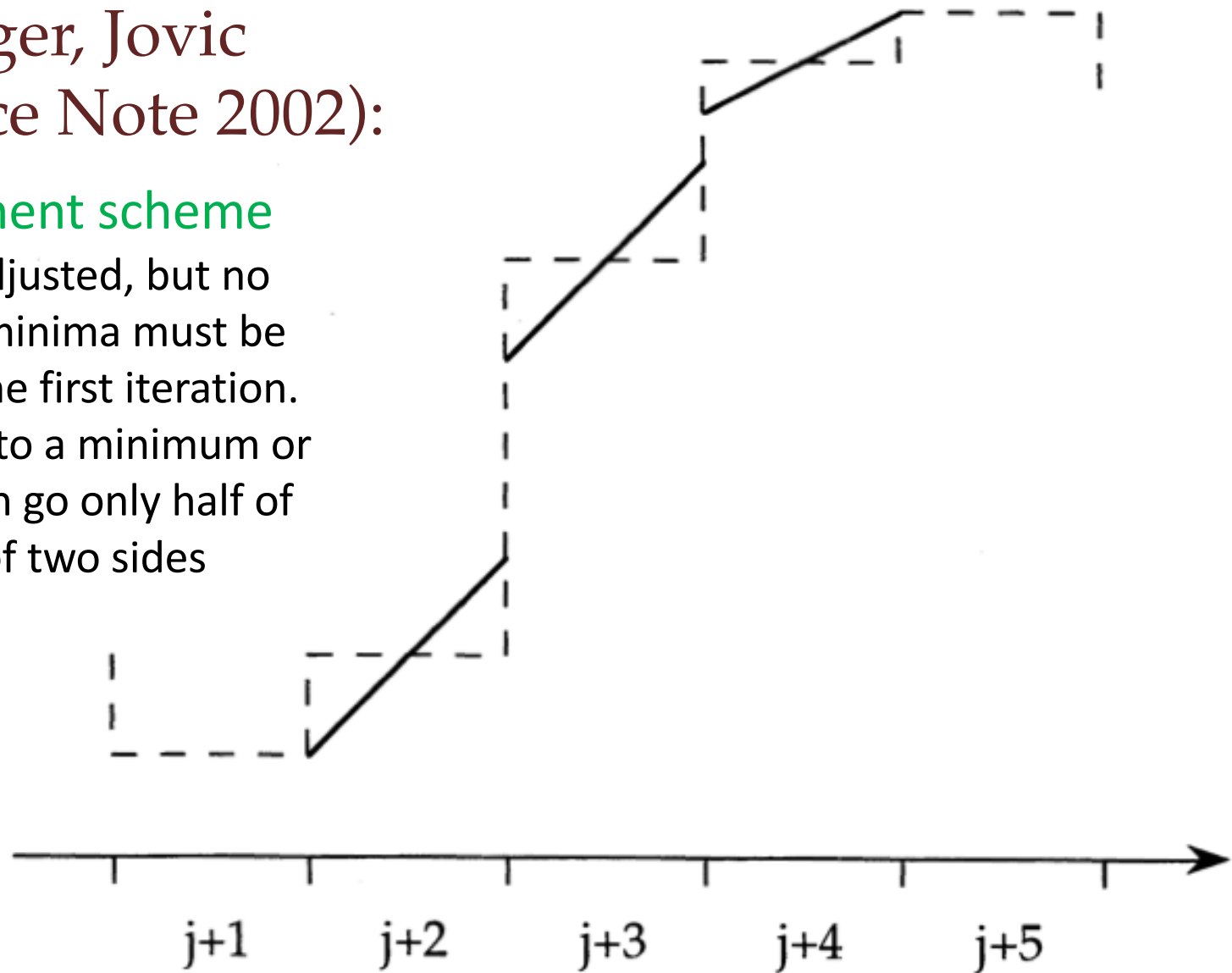


Figure 1. An example of the Eta iterative slope adjustment algorithm. The initial distribution is illustrated by the dashed line, with slopes in all five zones shown equal to zero. Slopes resulting from the first iteration are shown by the solid lines. See text for additional detail.

Minmod limiter:

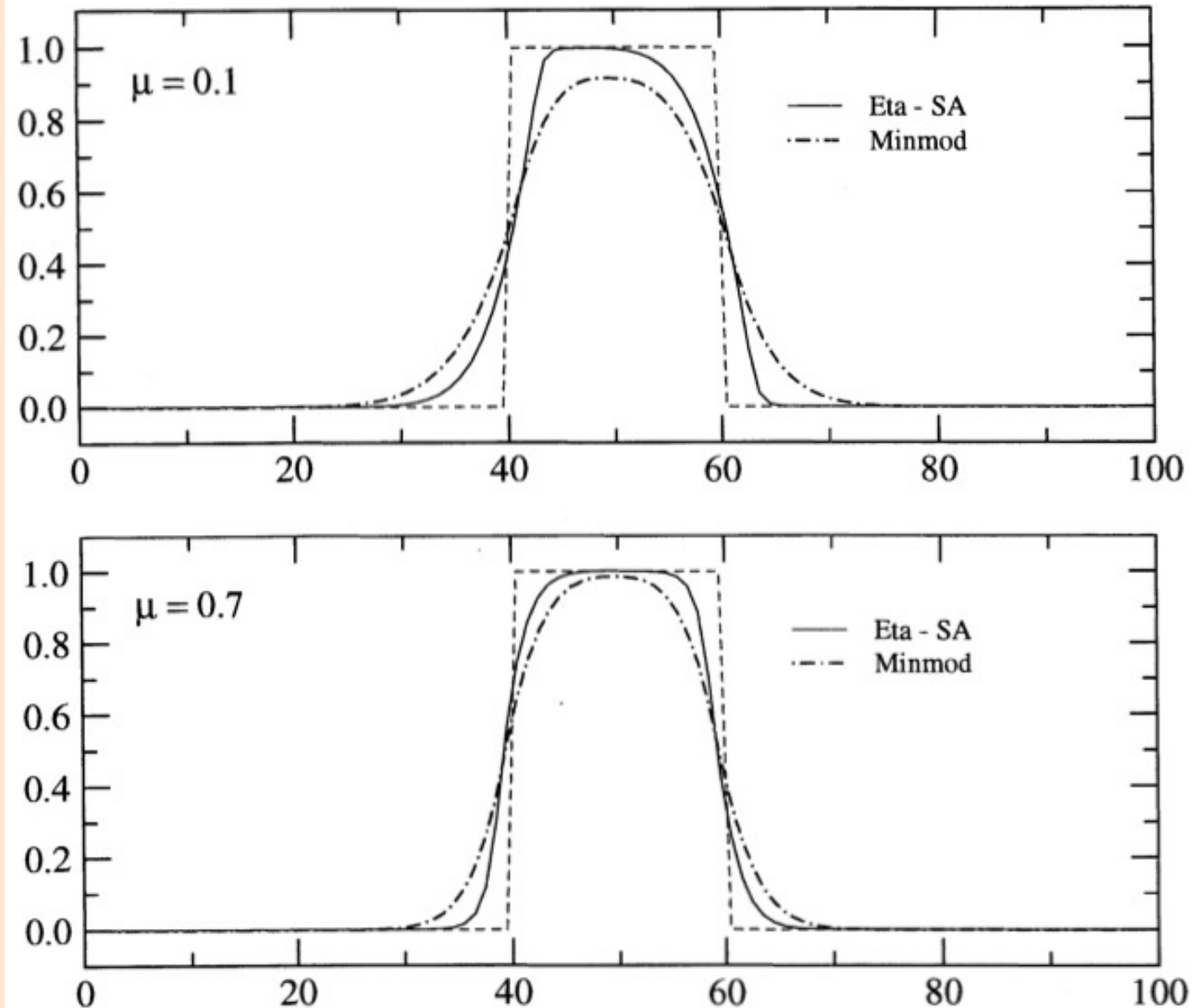
$$C = C(r),$$

$$r \equiv \frac{q_j - q_{j-1}}{q_{j+1} - q_j}$$

$$C(r) = \max\langle 0, \min(1, r) \rangle$$

defines slope to be that of the **smaller**, in absolute value, of the two boundary values of $\Delta q / \Delta x$, unless q_j is an extremum in which case the slope is zero

(Durrant 1999, and also 2010, Fig. 5.16.)



After two translations of the true solution across the domain

Figure 4. Same as Fig. 2, except for the Eta slope-adjustment scheme results (SA, solid line) compared against those using the minmod slope limiter (dot-dashed line). See text for definitions of schemes.

Monotonized-centered limiter:

$$C(r) = \max\left\langle 0, \min\left(2r, \frac{1+r}{2}, 2\right) \right\rangle$$

(also van Leer 1977)
algebraic average of
the two boundary
slopes (same as
using a centered
scheme), unless this
violates the
monotonicity
condition in which
case they are
reduced to the
extent required. If
however q_j is an
extremum the slope
is again set to zero

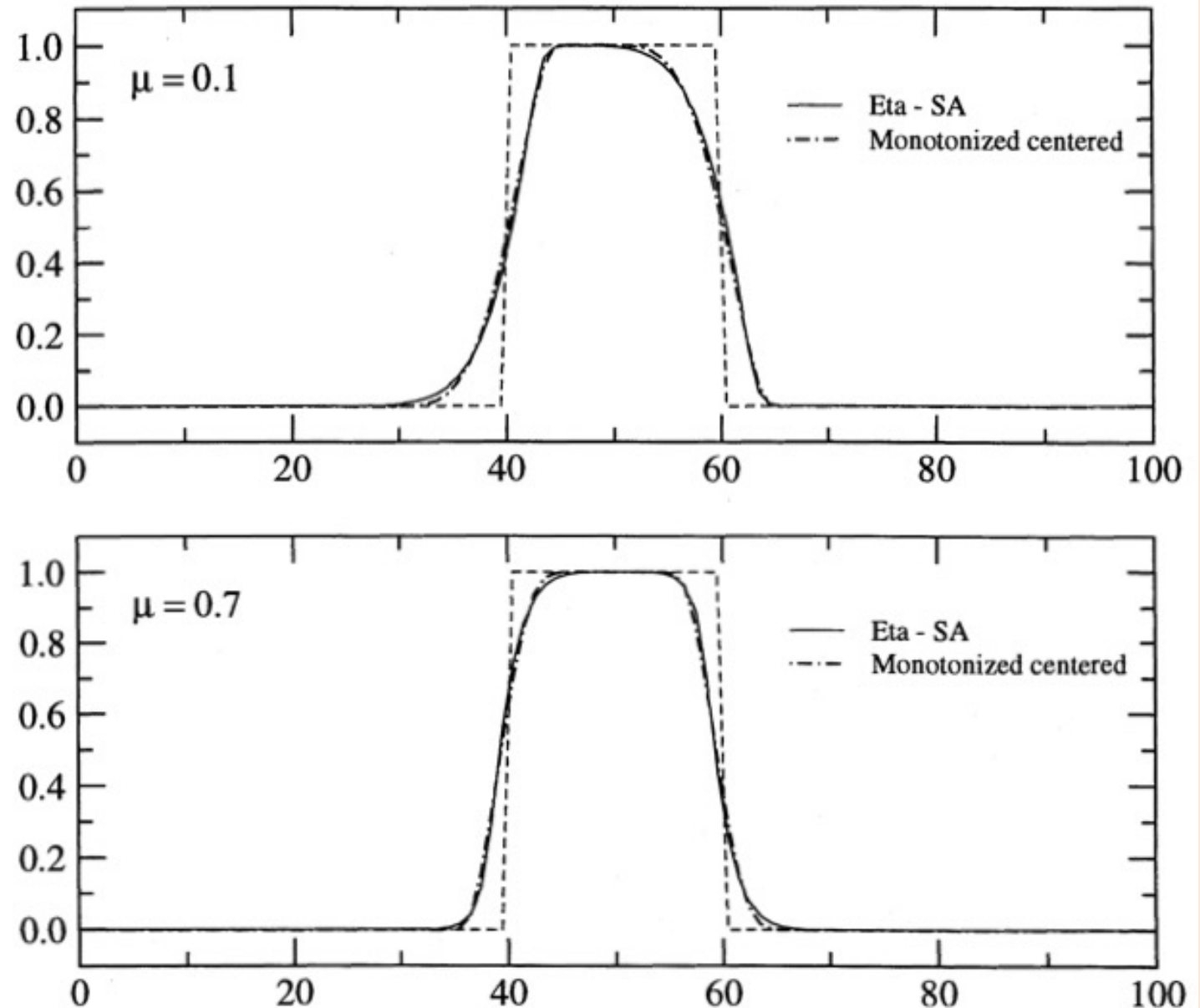


Figure 6. Same as Fig. 2, except for the Eta slope-adjustment scheme results (SA, solid line) compared against those using the monotonized centered slope limiter (dot-dashed line). See text for definitions of schemes.

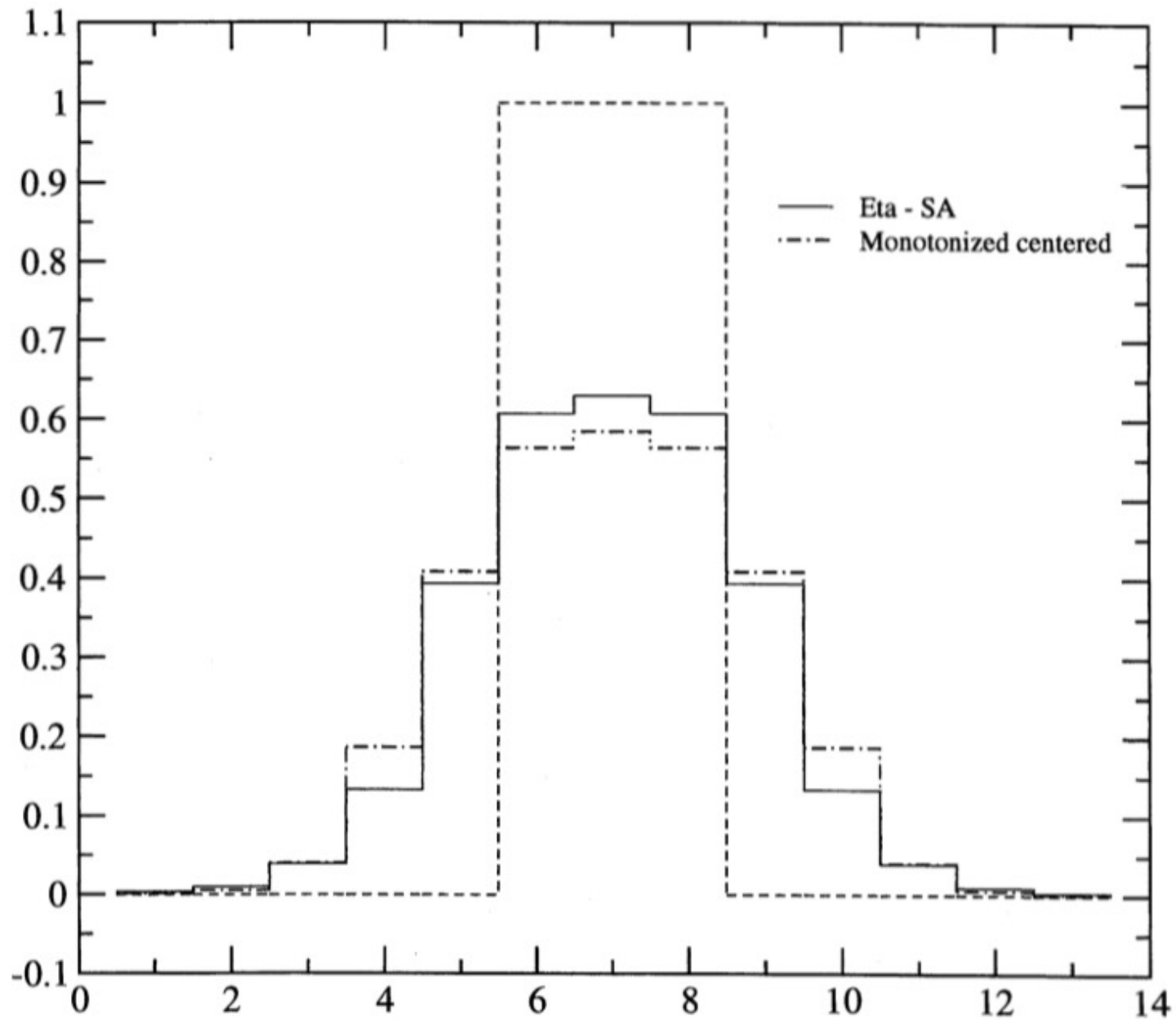


Figure 8. Same as Fig. 6, except for a "narrow" square wave initial distribution, spanning 3 zones, and a 13 zone domain.

Takacs' 3rd order scheme

(3rd order when its parameter α is a given function of μ)

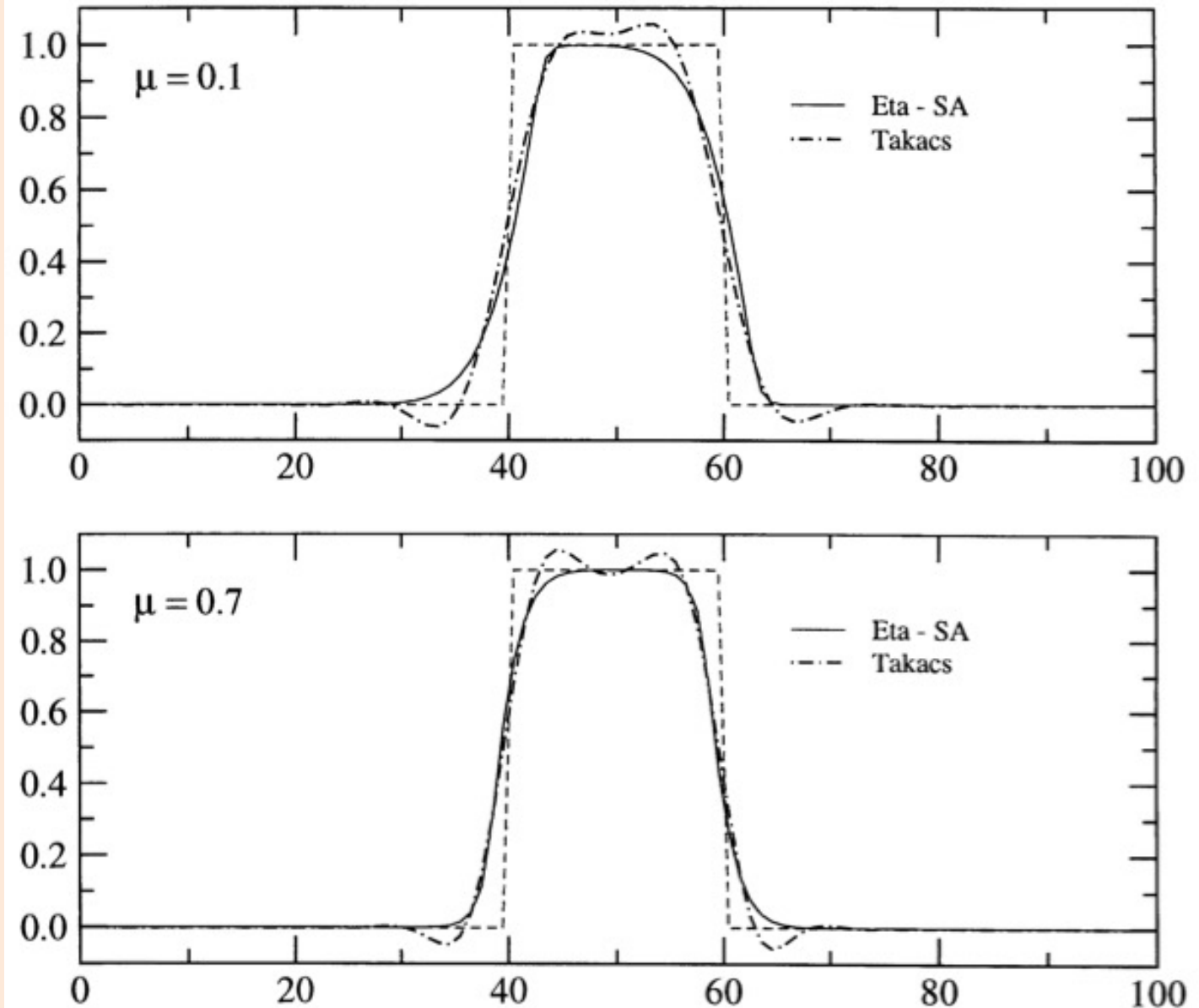


Figure 9. Same as Fig. 2, except for the Eta slope-adjustment scheme results (SA, solid line) compared against those using the Takacs (1985) third-order "minimized dissipation and dispersion errors" scheme (dot-dashed line). See text for definitions of schemes.

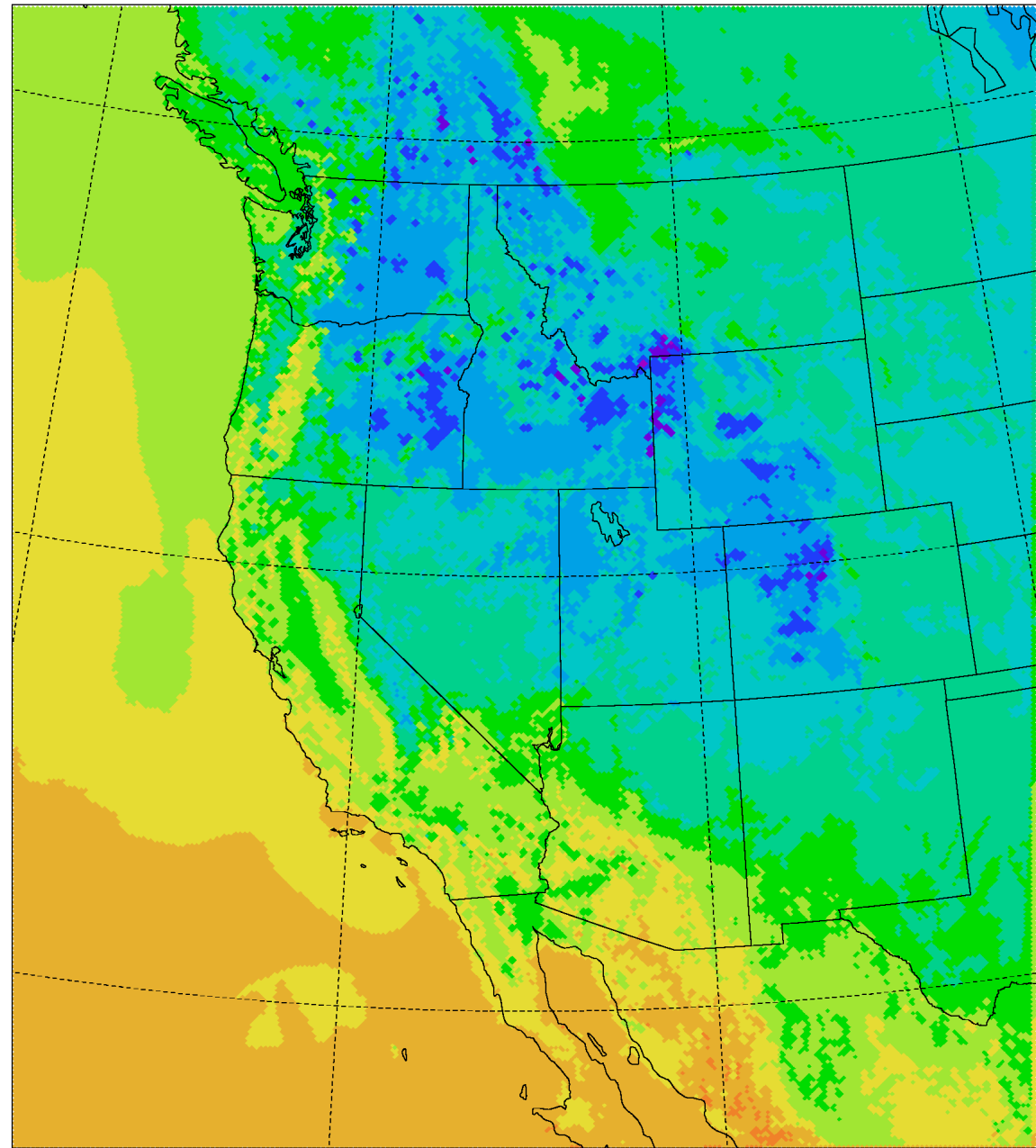
A still more ambitious scheme:

Rančić M., 1992: Semi-Lagrangian **piecewise bi-parabolic** scheme for two-dimensional horizontal advection of a passive scalar. *Mon. Wea. Rev.*, **120**, 1394-1406.

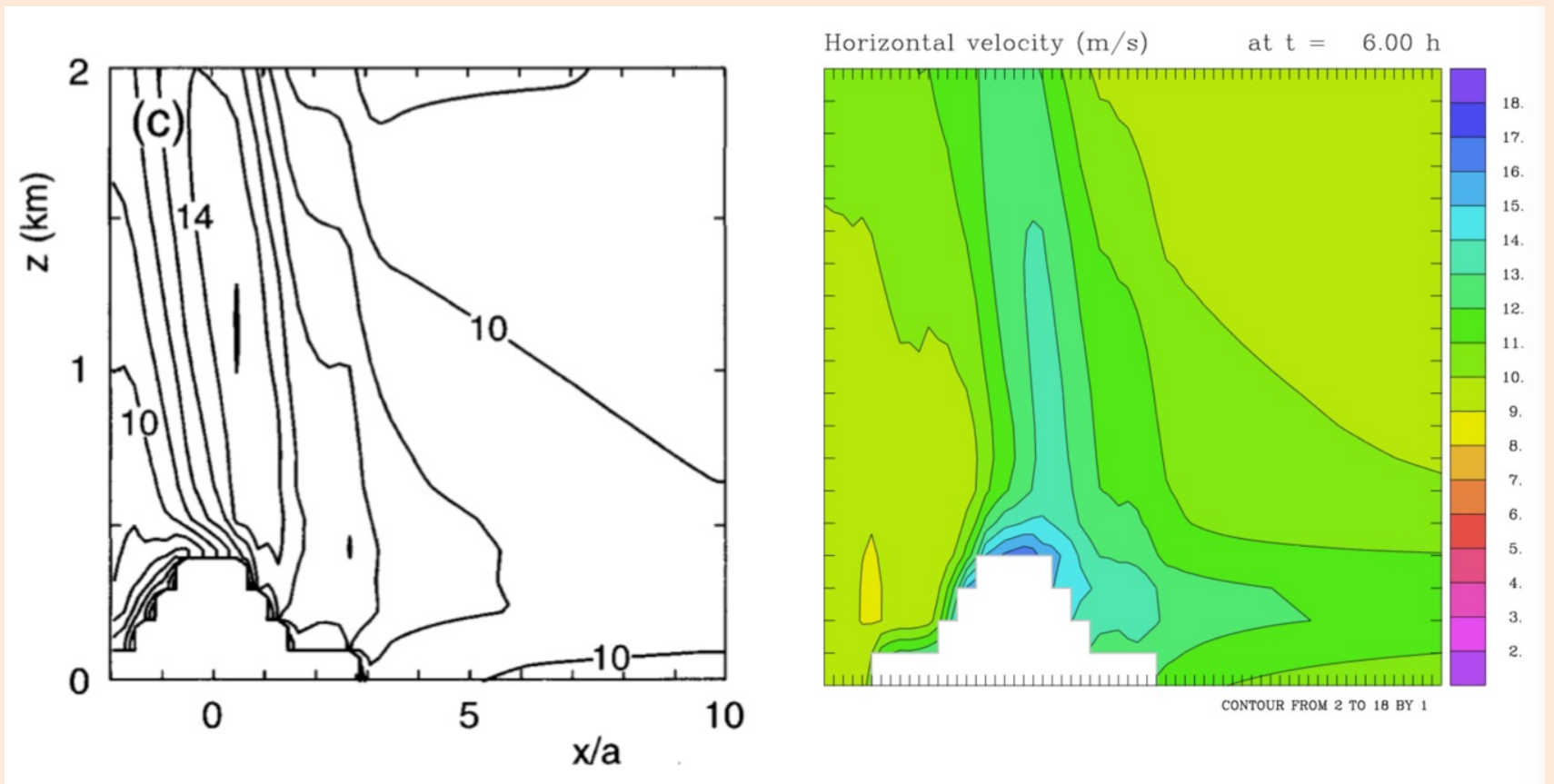
With finite difference scheme of slide (30) replaced by the Lagrangean slantwise advection, and the van Leer type SA scheme for vertical advections of all prognostic variables, 48-h lowest T values now

VALID 11 Dec 2005 12Z Sunday

20051209 12UTC 48h fcst



And the
Gallus-
Klemp
problem:

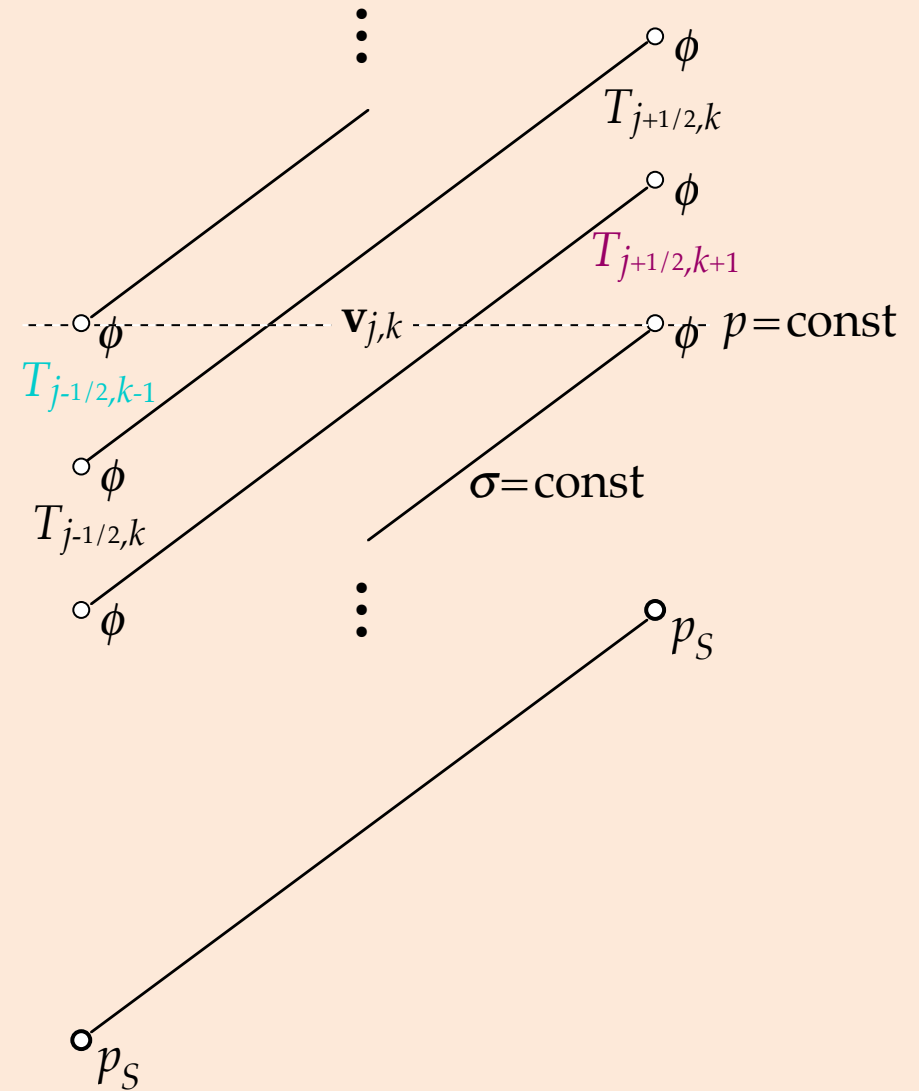


Simulation of the Gallus-Klemp experiment with the Eta code, plot (c) of Fig. 6 of Gallus and Klemp (2000), left, using the sloping steps Eta code allowing for velocities at slopes in the horizontal diffusion scheme, right. From Mesinger and Veljovic (Meteor Atmos Phys, 2017).

The eta vertical coordinate

Terrain-following coordinates:
pressure gradient force has
problems!

Continuous case:
PGF should depend on,
and only on,
variables from the ground
up to the $p = \text{const}$ surface:



Accuracy

of a model, ran using real data IC

Issues:

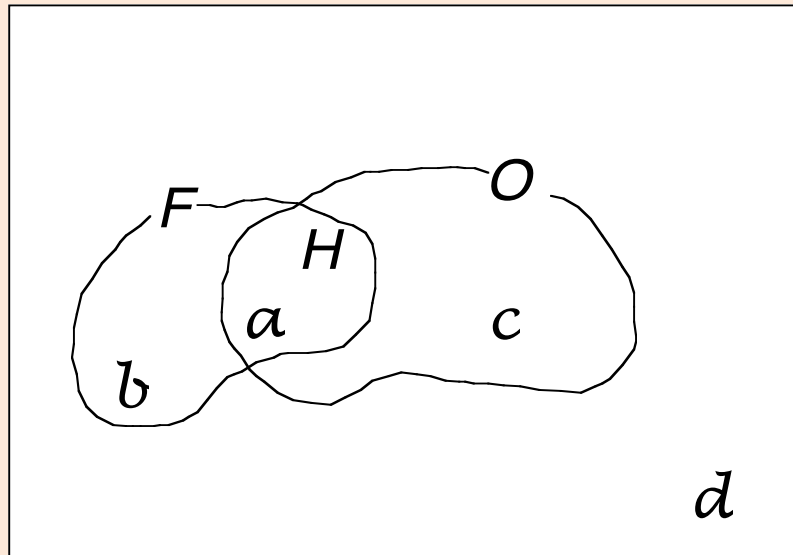
Atmosphere is chaotic,

Results depend on data
assimilation system / the IC

Impacts of both are avoided if we
drive our limited area "test
model" by ICs and LBCs of an
ensemble of a global model

Accuracy of the jet stream position

Forecast, Hits, and Observed (F , H , O) area,
or number of model grid boxes:



Many verification scores.

One:

$$ETS = \frac{H - E(H)}{F + O - H - E(H)}$$

“Equitable Threat Score”

or, Gilbert (1884 !) Skill Score

$$\text{Bias} = F/O$$

ETS corrected (adjusted) for bias: ETS_a :

Mesinger F, 2008: Bias adjusted precipitation threat scores. *Adv. Geosci.*, **16**, 137-143 ([open access](#)).

ECMWF once a week runs a 51
member ensemble forecast 32
days ahead

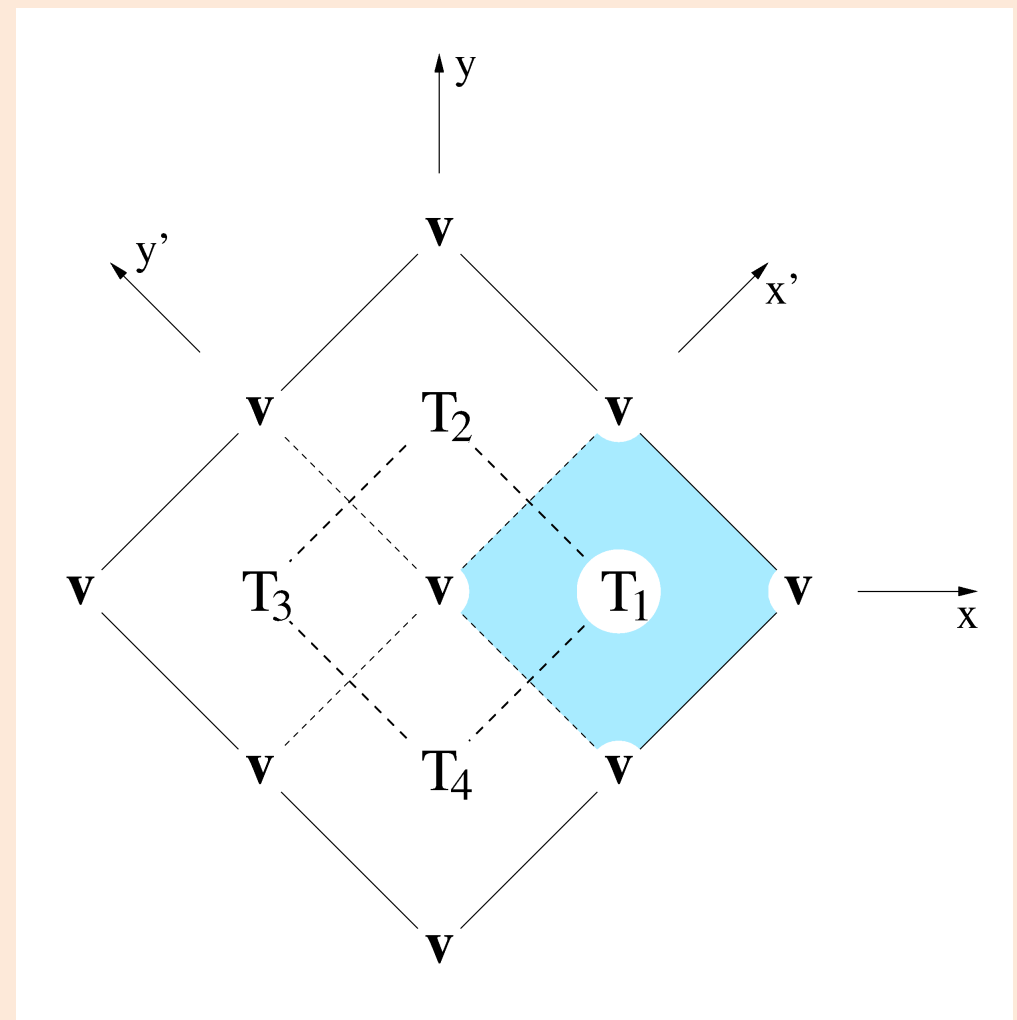
Mesinger F, Chou SC, Gomes J, Jovic D, Bastos P, Bustamante JF, Lazic L, Lyra AA, Morelli S, Ristic I, Veljovic K (2012) An upgraded version of the Eta model. *Meteorol Atmos Phys* **116**, 63–79.
doi:10.1007/s00703-012-0182-z

Mesinger, F, Veljovic K (2017) Eta vs. sigma: Review of past results, Gallus-Klemp test, and large-scale wind skill in ensemble experiments. *Meteorol Atmos Phys*, **129**, 573-593,
doi:10.1007/s00703-016-0496-3

Horizontal treatment, 3D

Case #1: topography of box 1 is higher than those of 2, 3, and 4; “Slope 1”

Inside the central v box, topography descends from the center of T_1 box down by one layer thickness, linearly, to the centers of T_2 , T_3 and T_4



Acknowledgements: Dušan Jović, Jorge Gomes, Ivan Ristić

How are grid cell values of topography obtained ?

Chop up each cell into $n \times n$ sub-cells;

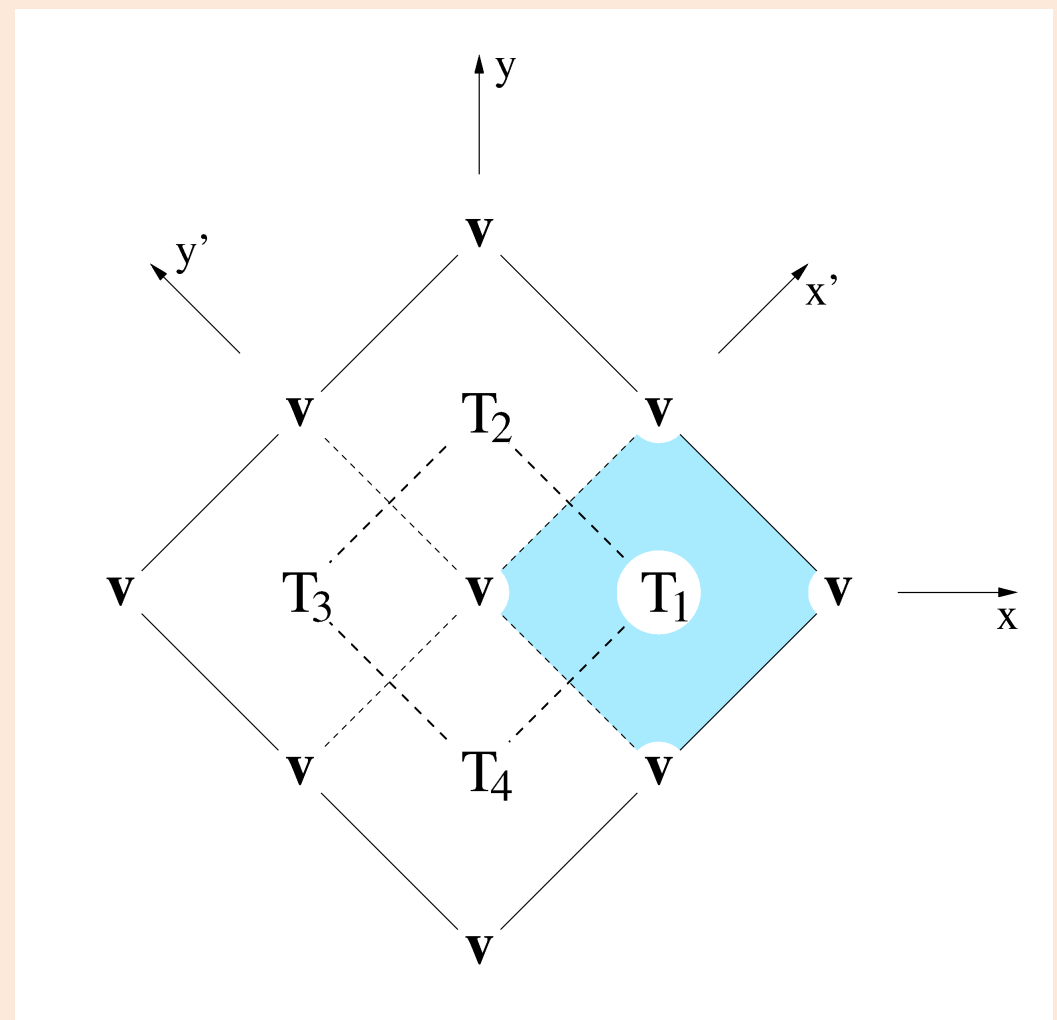
Obtain each sub-cell mean value;

Obtain **mean** h_m and **silhouette cell** value, round off to discrete interface value;

Choose one depending on Laplacian h_m ;

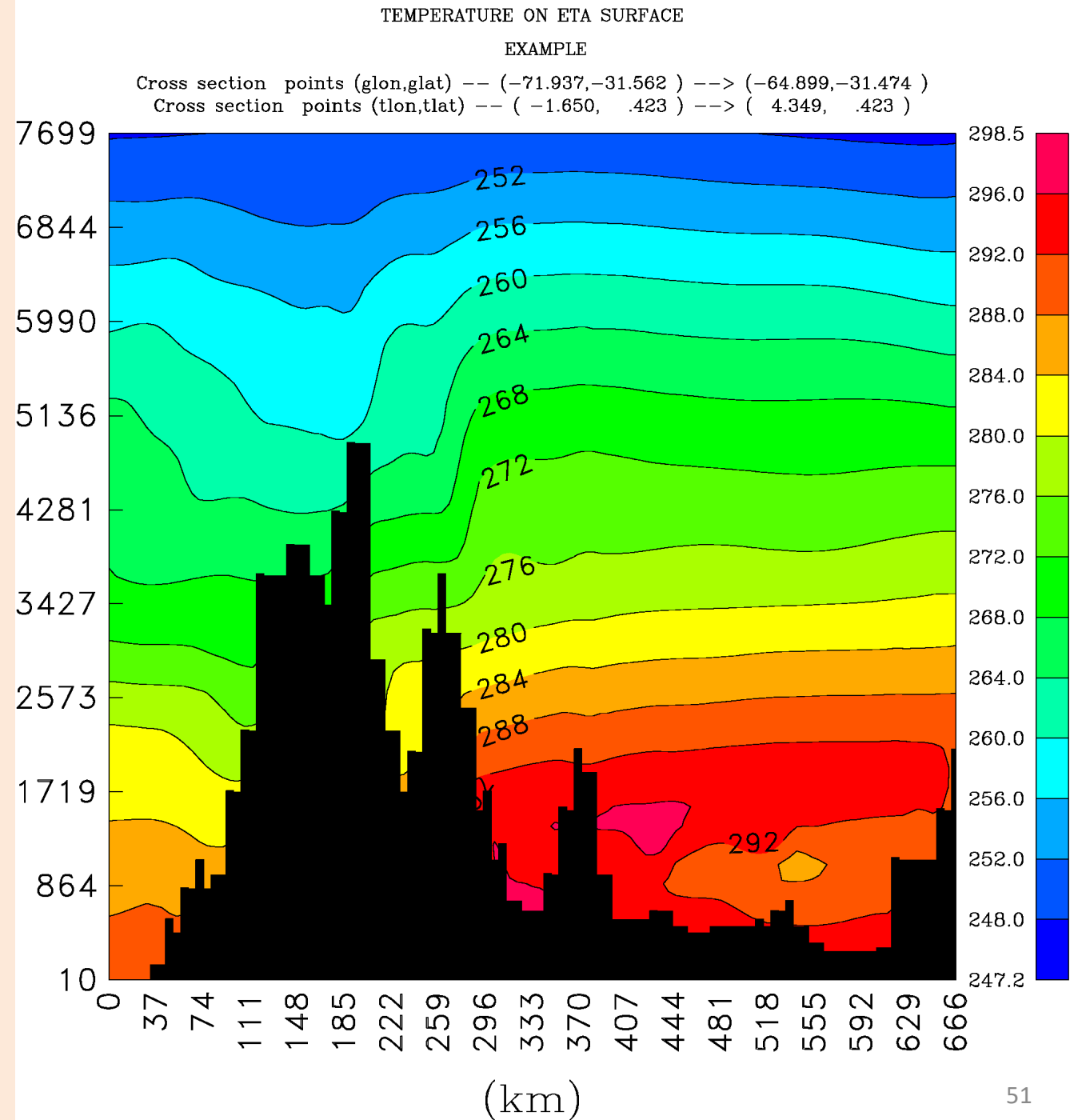
Remove basins with all corner winds blocked;

Some more common sense rules but **no smoothing**



8 km
horizontal
resolution,
W/E profile at the
latitude of about
the highest
elevation of the
Andes

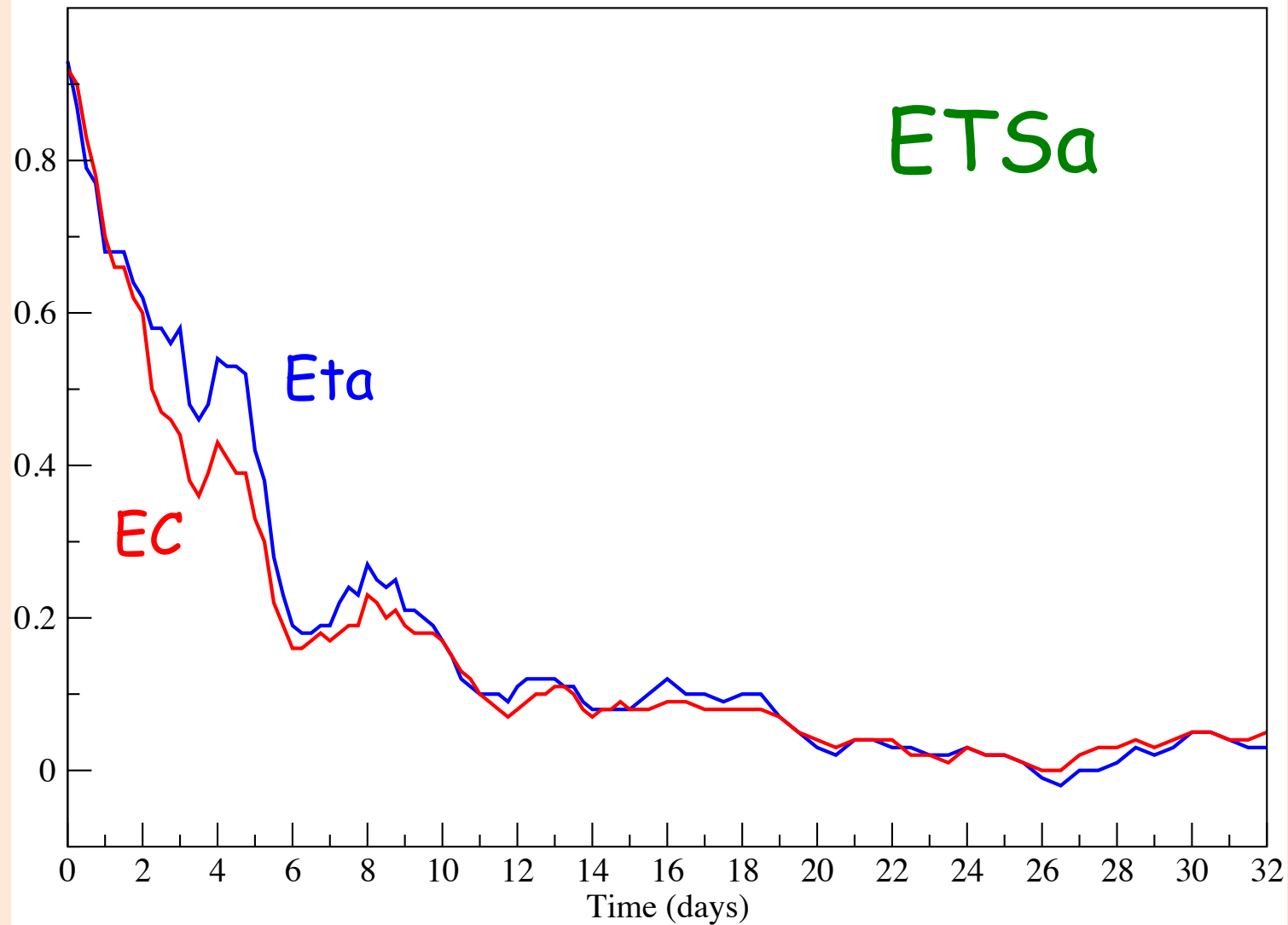
NCAR graphics,
no cell values
smoothing



Verification results

21 ensemble members

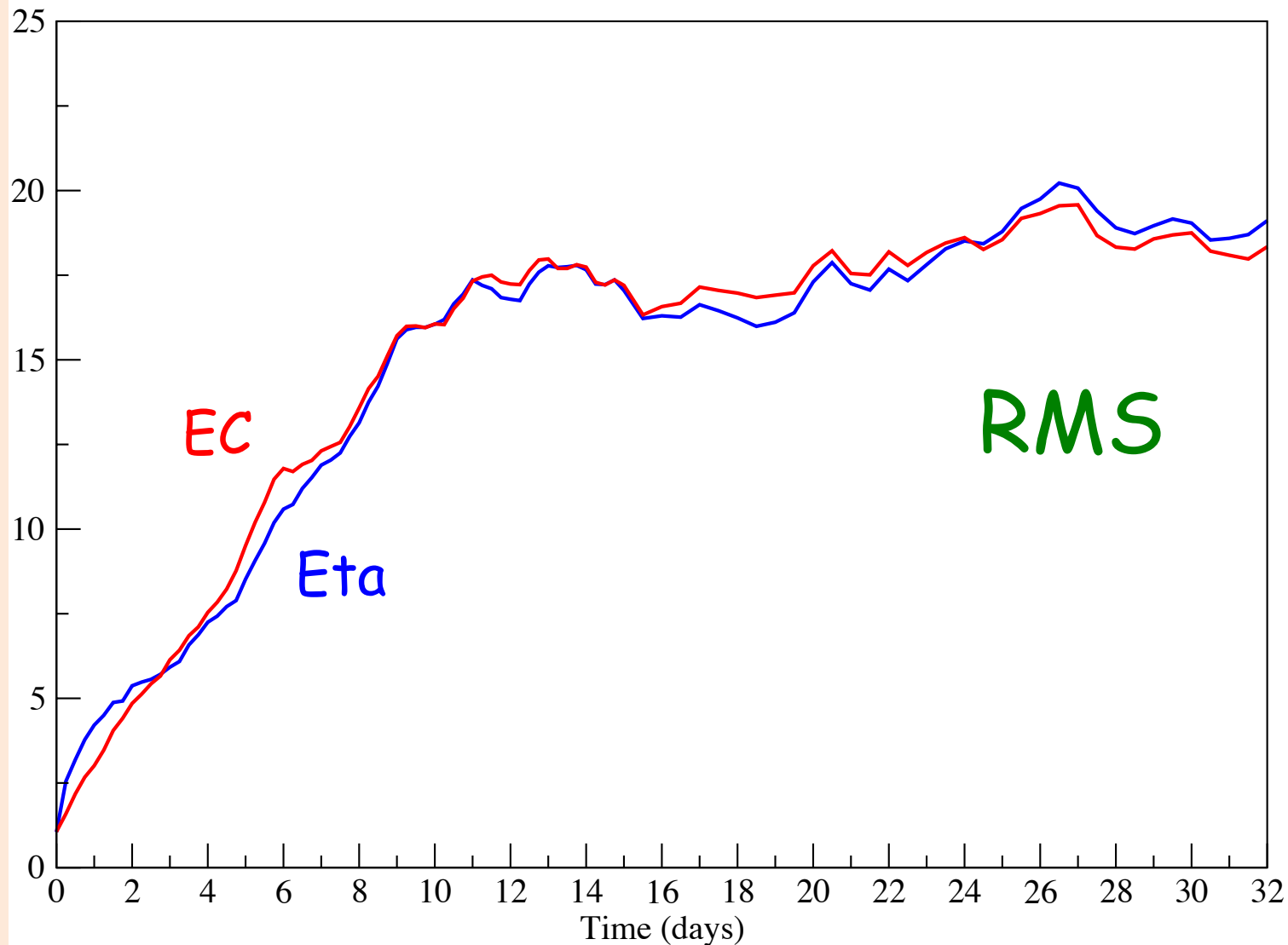
Cumulative ETSa, 21 ensemble members



Bias
adjusted
ETS scores
of wind
speeds > 45
m s⁻¹, at 250
hPa, with
respect to
ECMWF
analyses

ETSa:
More is
better !

Cumulative RMS difference, 21 members



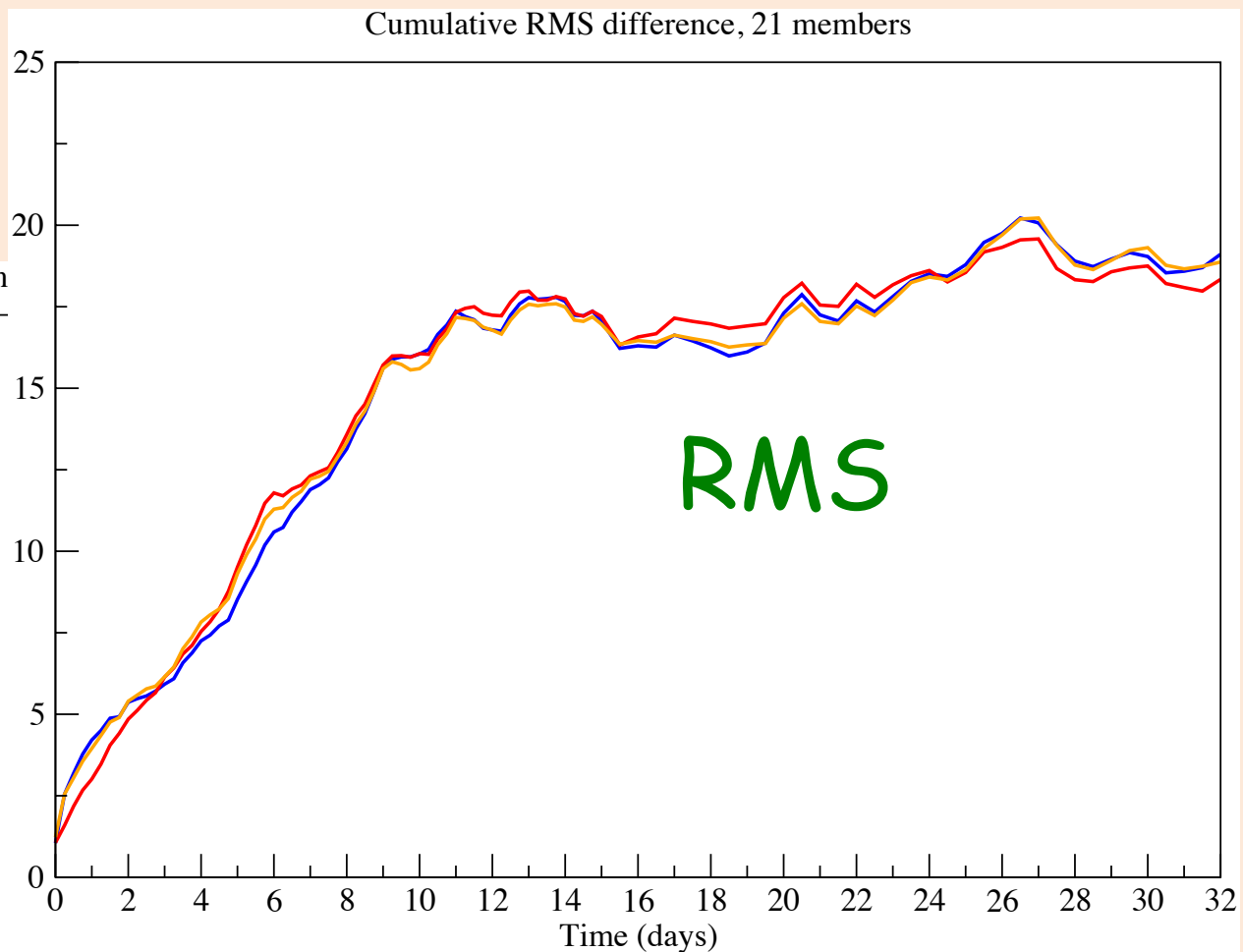
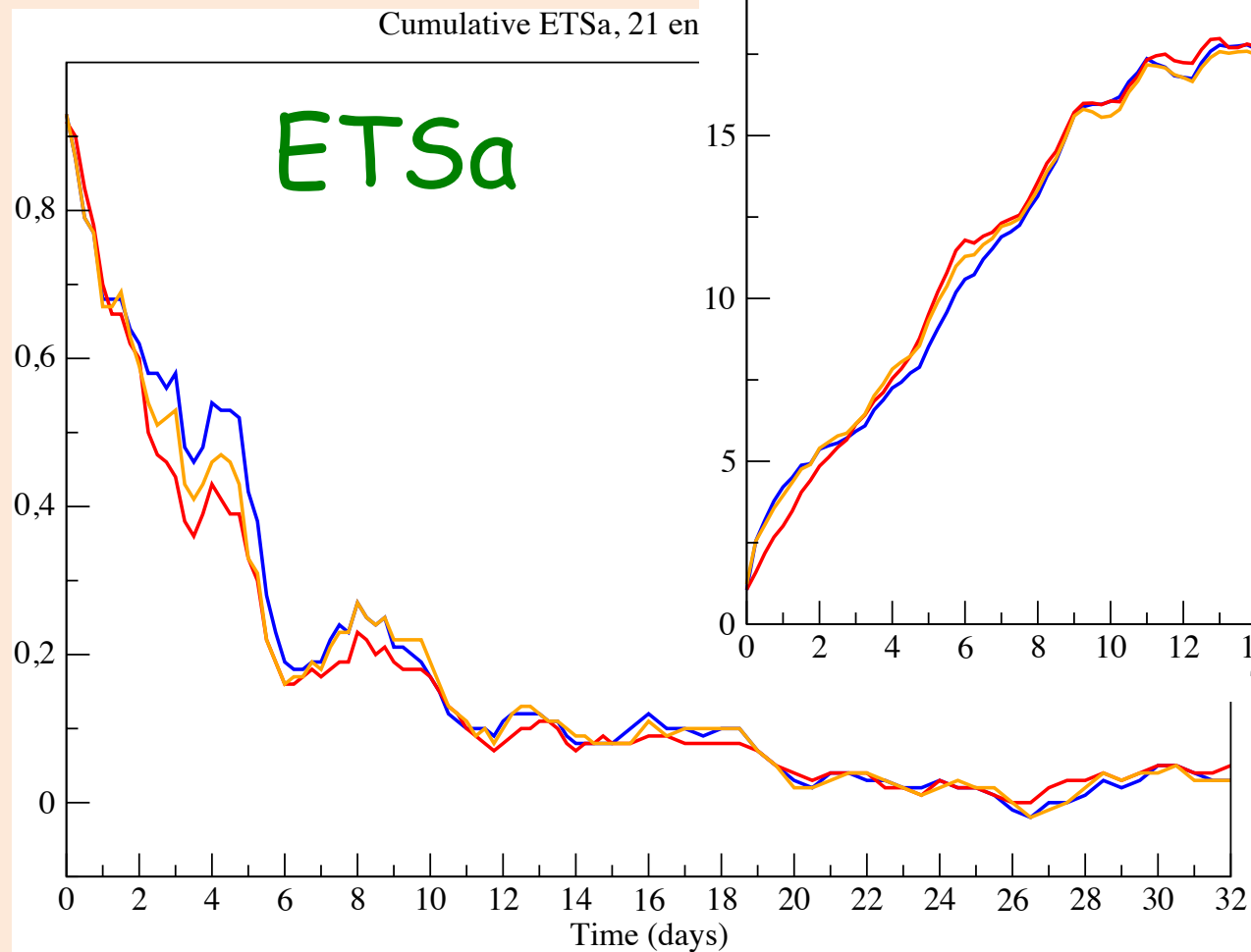
RMS wind difference of 250 hPa winds, with respect to ECMWF analyses

RMS:
Less is better!

What ingredient of the Eta is responsible for the advantage in scores ?

(It is **not** resolution, the first 10 days resolution of two models was about the same)

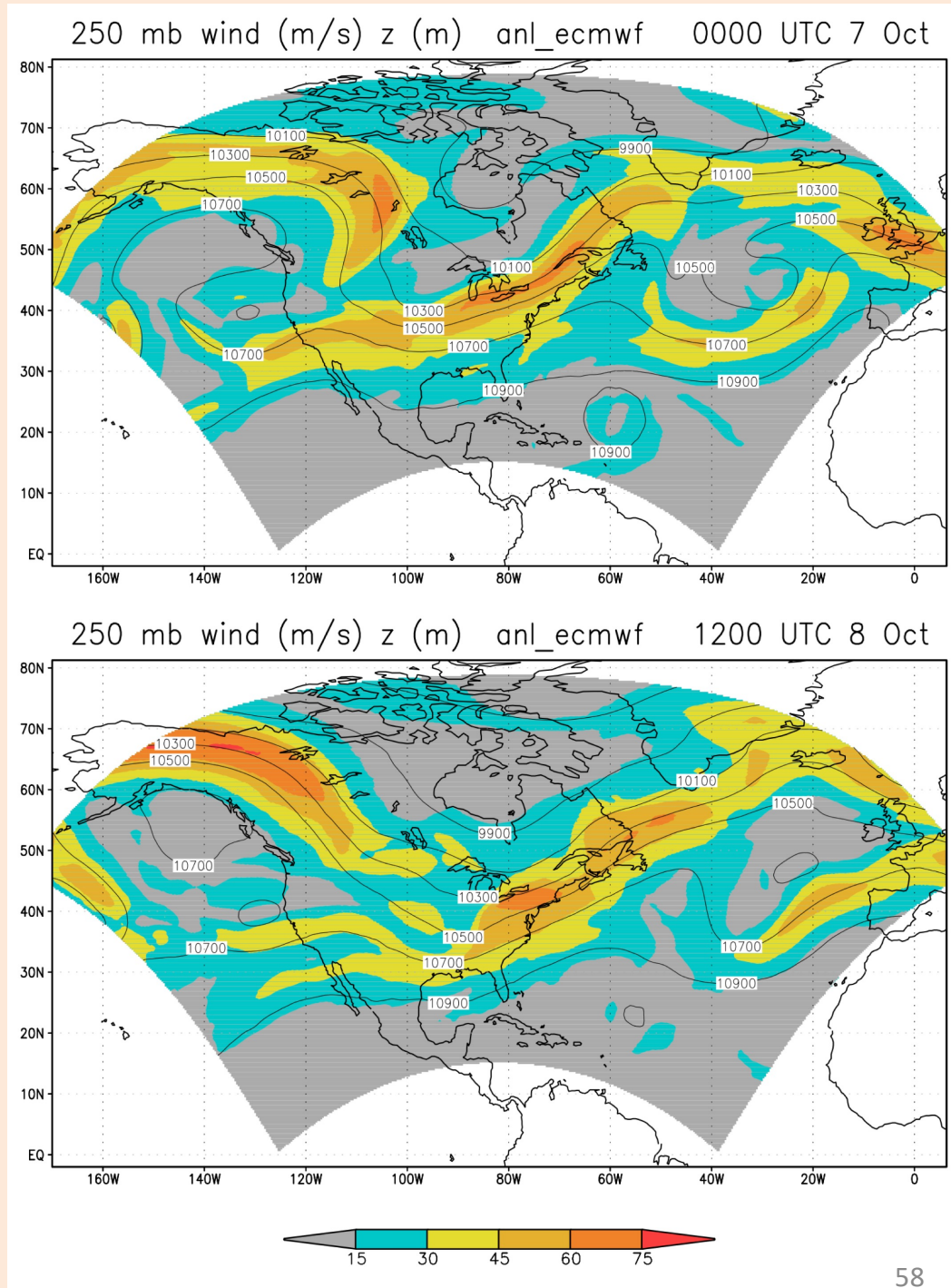
21 members ran
using Eta/sigma:



What was going
on at about day
2-6 time ?

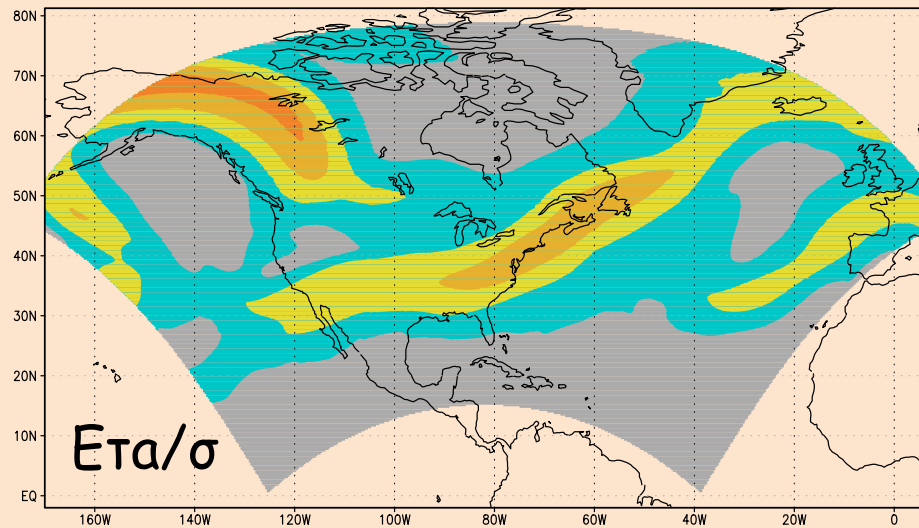
What was going on at about day 2-6 time?

The plot times correspond to **day 3.0,** and **4.5,** respectively, of the plots of the two preceding slides

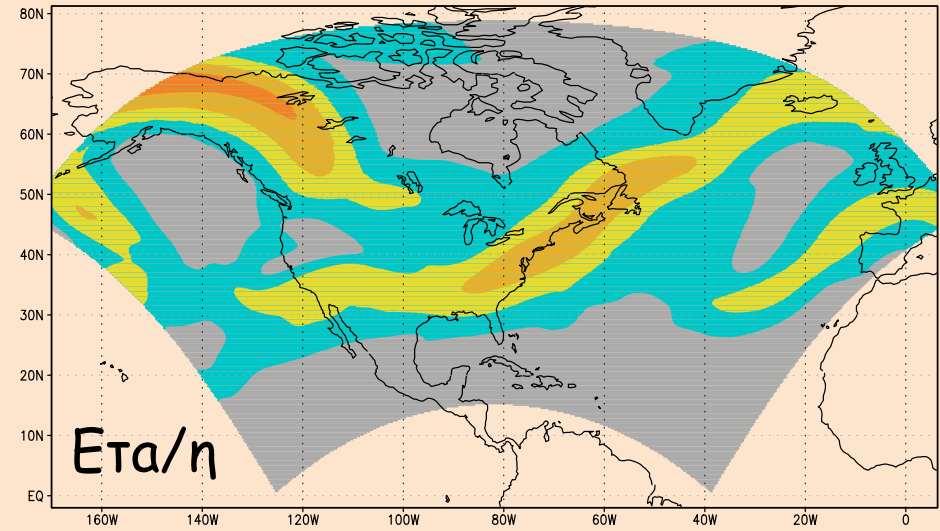


Why was the Eta more accurate at
this time ?

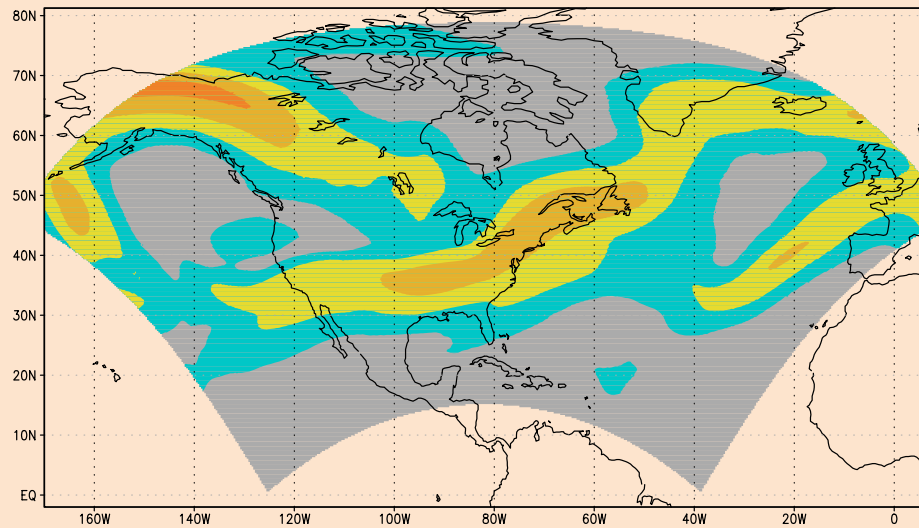
250 mb wind (m/s) Eta_s ensemble hr=108



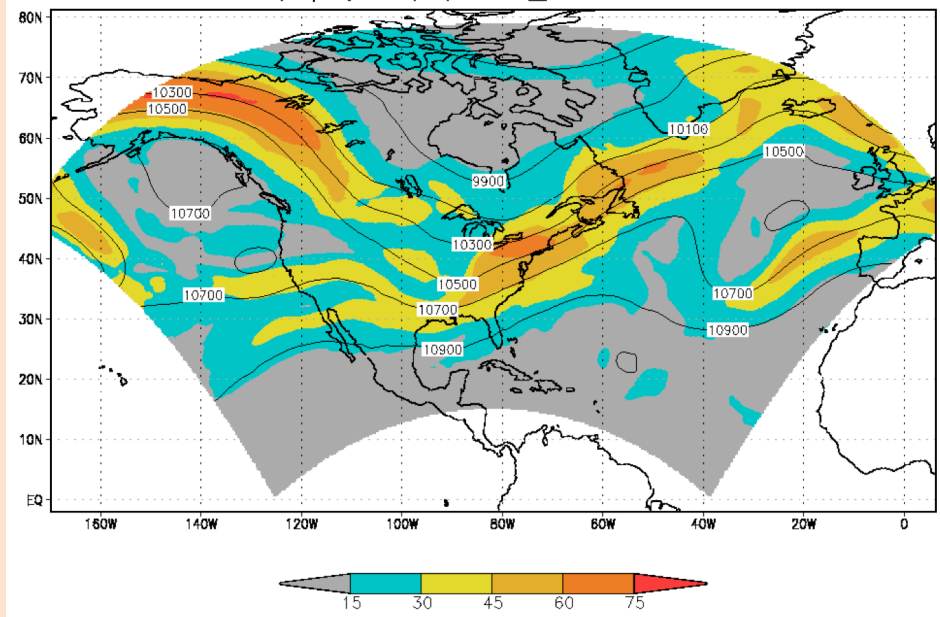
250 mb wind (m/s) Eta ensemble hr=108



250 mb wind (m/s) ECMWF ensemble hr=108



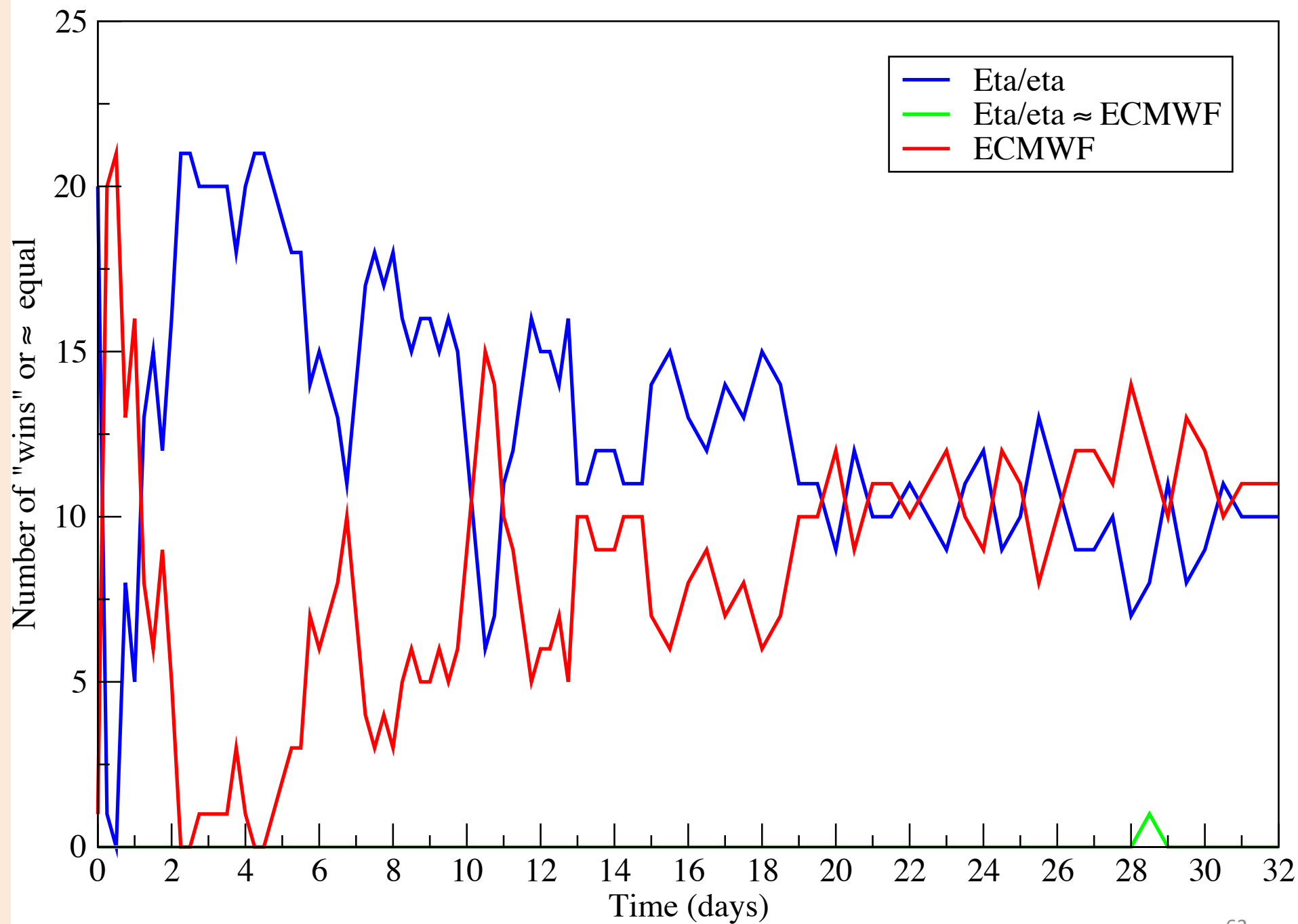
250 mb wind (m/s) z (m) anl_ecmwf 1200 UTC 8 Oct



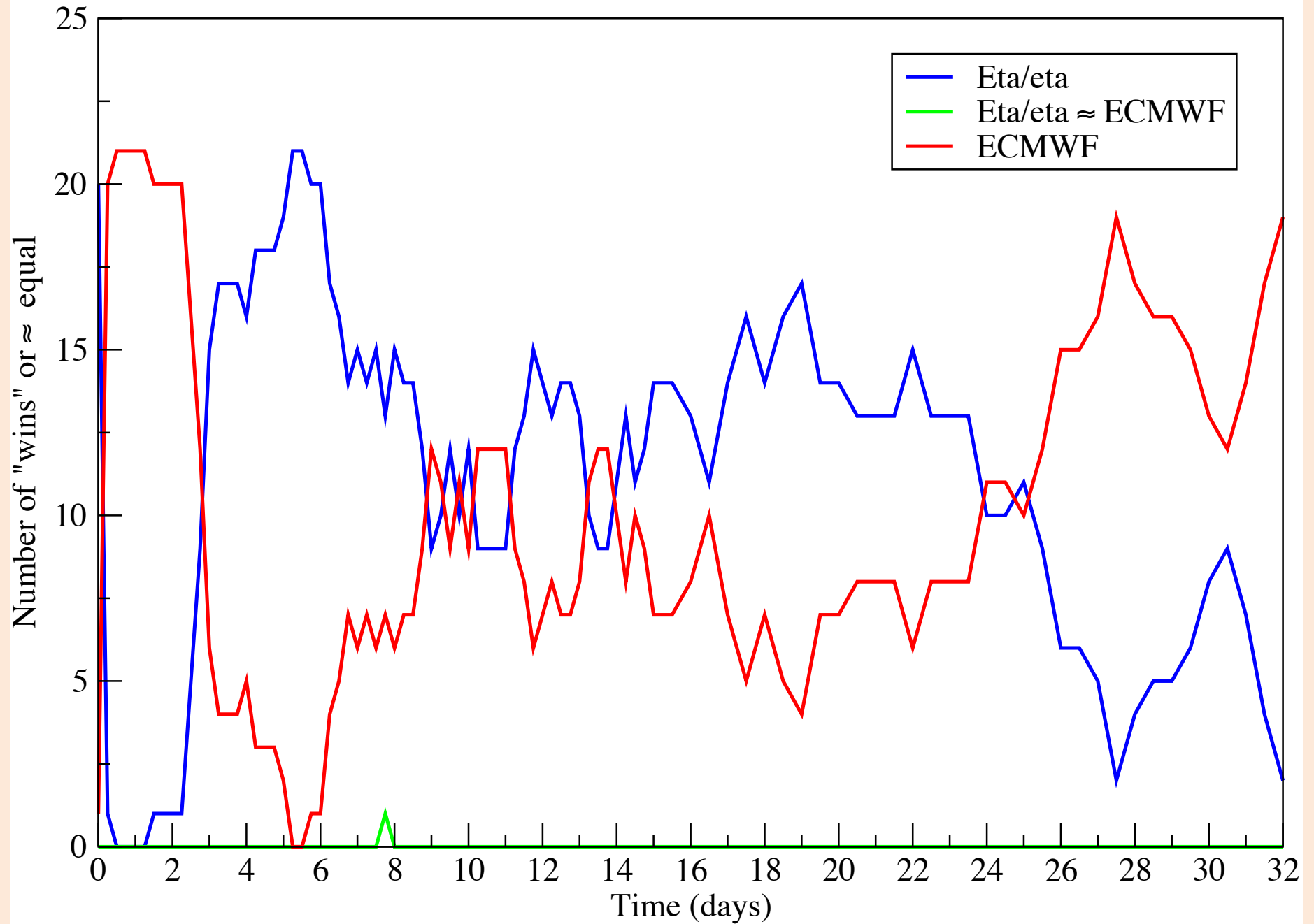
Ensemble average, 21 members, at 4.5 day time: Eta/sigma top left, Eta top right, EC driver bottom left, EC verification analysis bottom right.

Another way of comparing ensemble model skill
number of "wins"

Based on ETSa

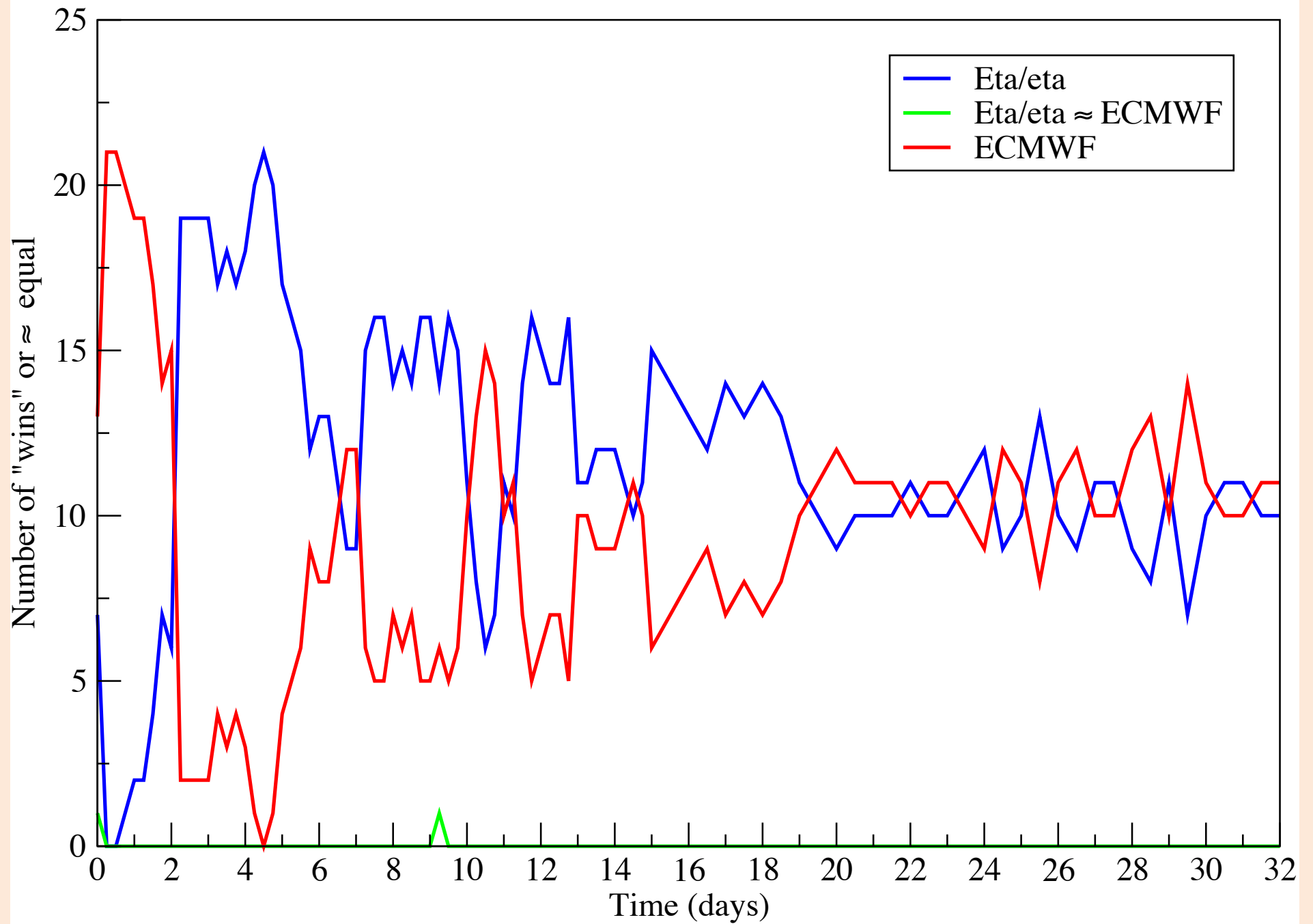


Based on RMS difference



Other ways of modifying ETS (or, GSS) aimed at reducing the possibility of artificially manipulating the score, in particular by increasing bias; and its non-informative behavior for rare events (Wilks 2011, p. 313); *symmetric extreme dependency score, SEDS*

Based on SEDS

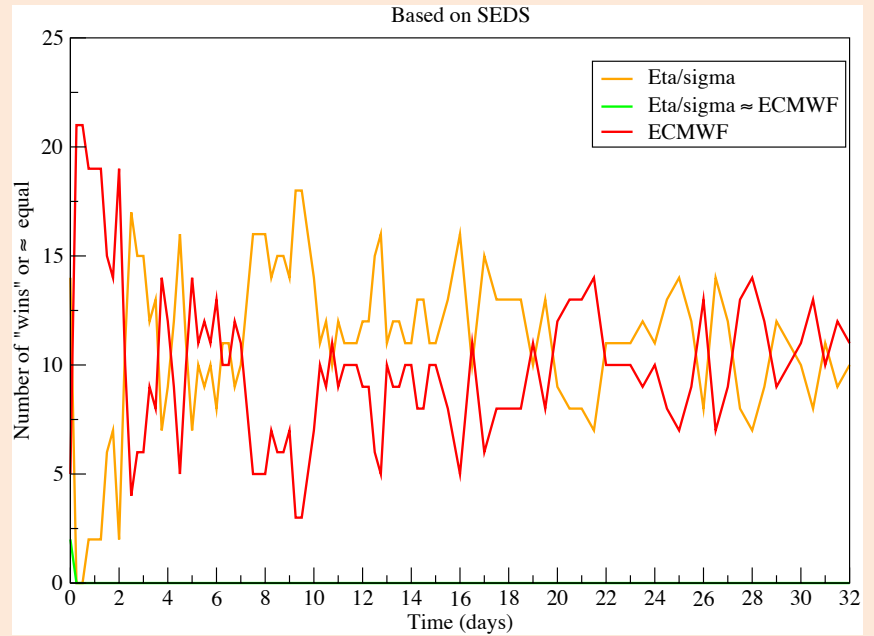
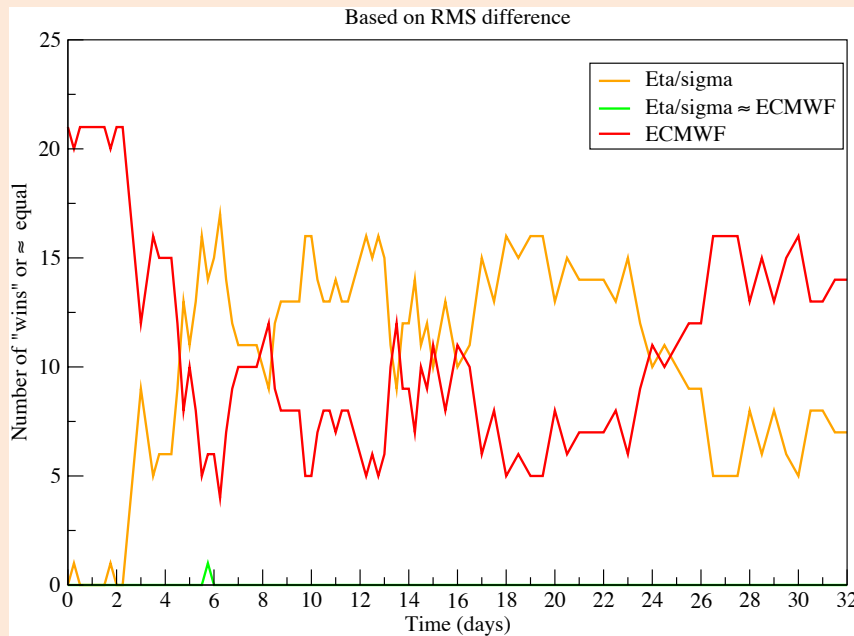
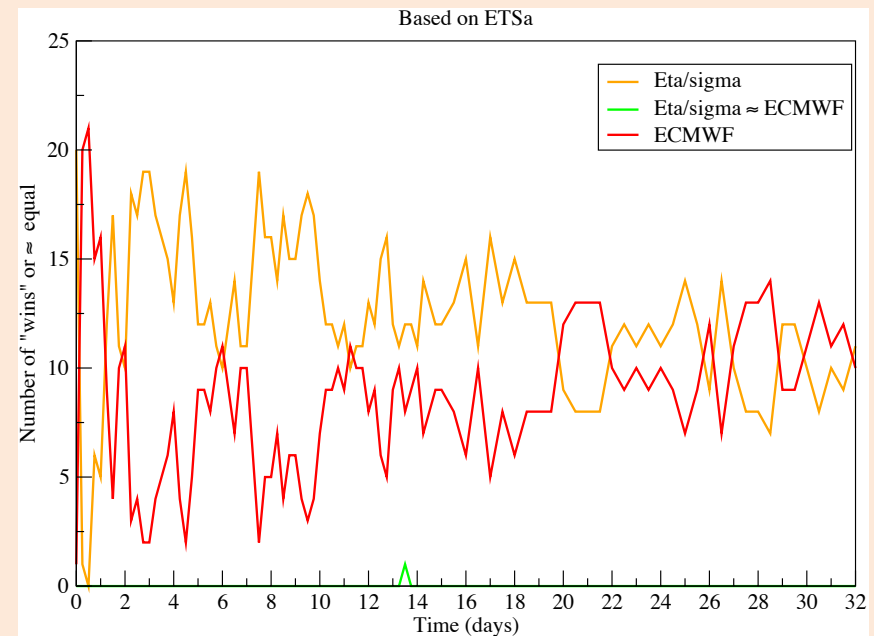


Using each of three accuracy scores, ETSa, RMS difference, and SEDS, at times ranging from 2.25 to 5.5 days, events occurred, 4, 2, 1 times, of **all 21** Eta members achieving better scores than their EC driver members

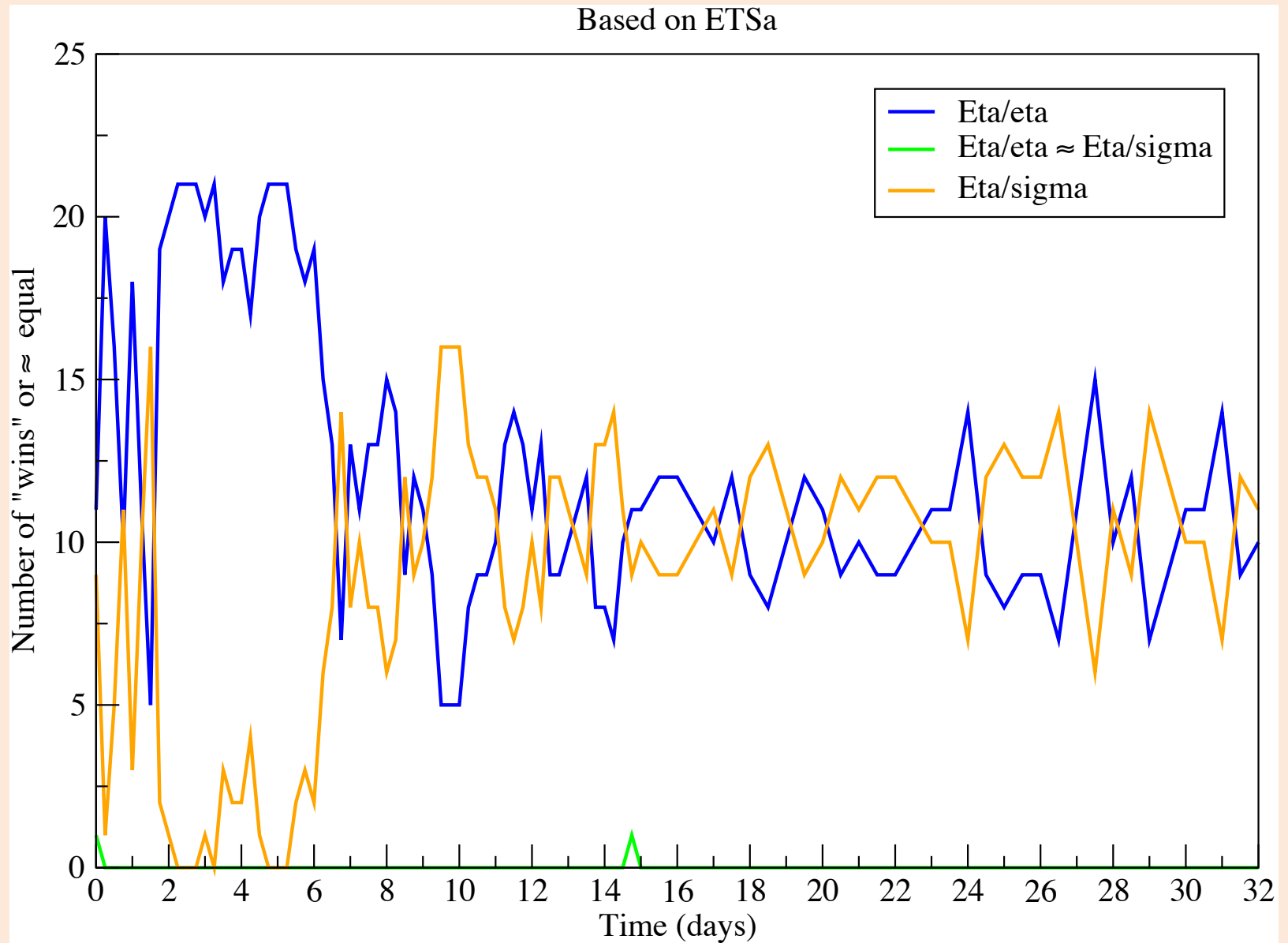
What happens if the Eta is switched to use sigma?

Using each of three accuracy scores, ETSa, RMS difference, and SEDS, at times ranging from 2.25 to 5.5 days, events occurred, 4, 2, 1 times, of **all 21** Eta members achieving better scores than their EC driver members

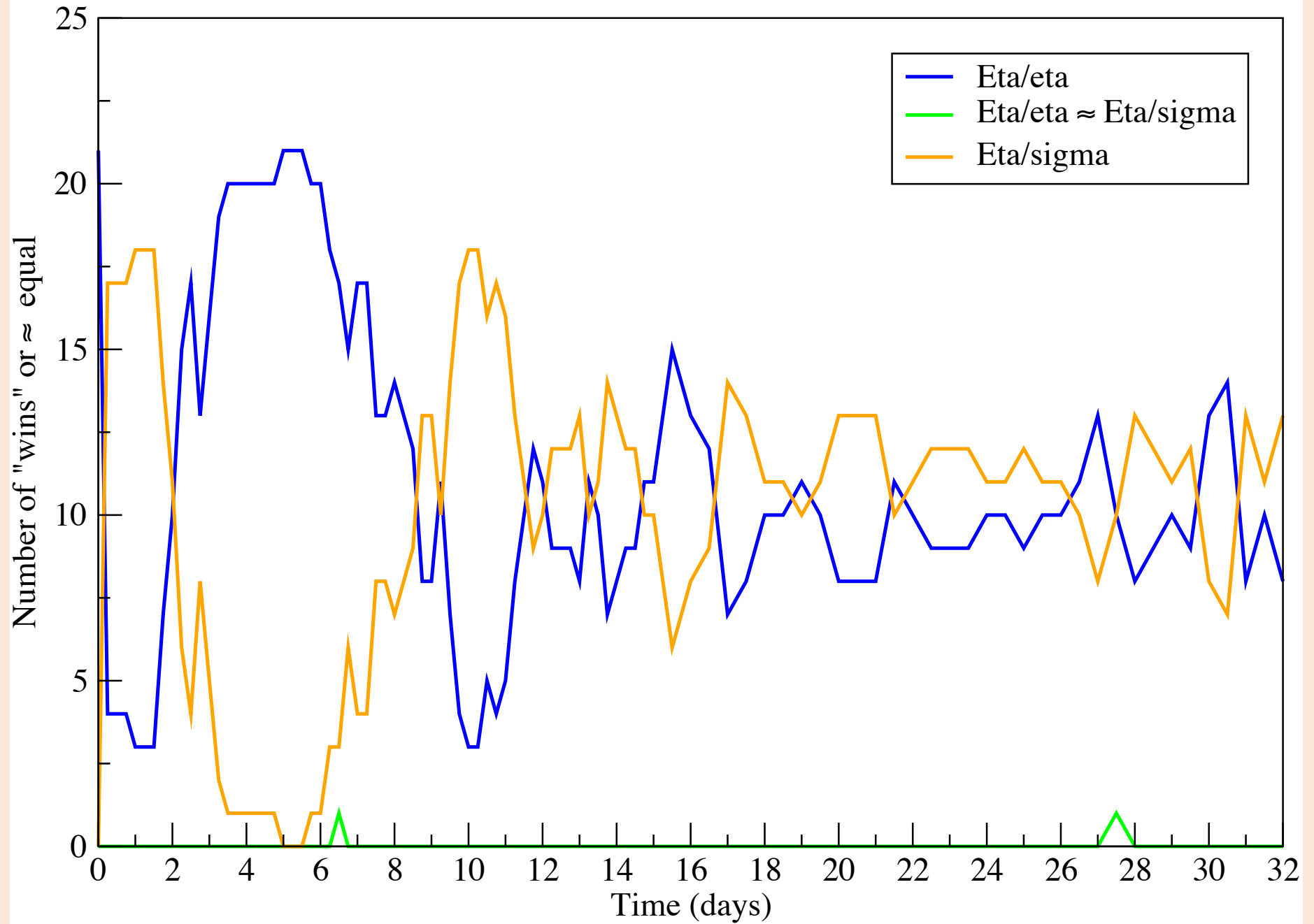
What happens if the Eta is switched to use sigma?



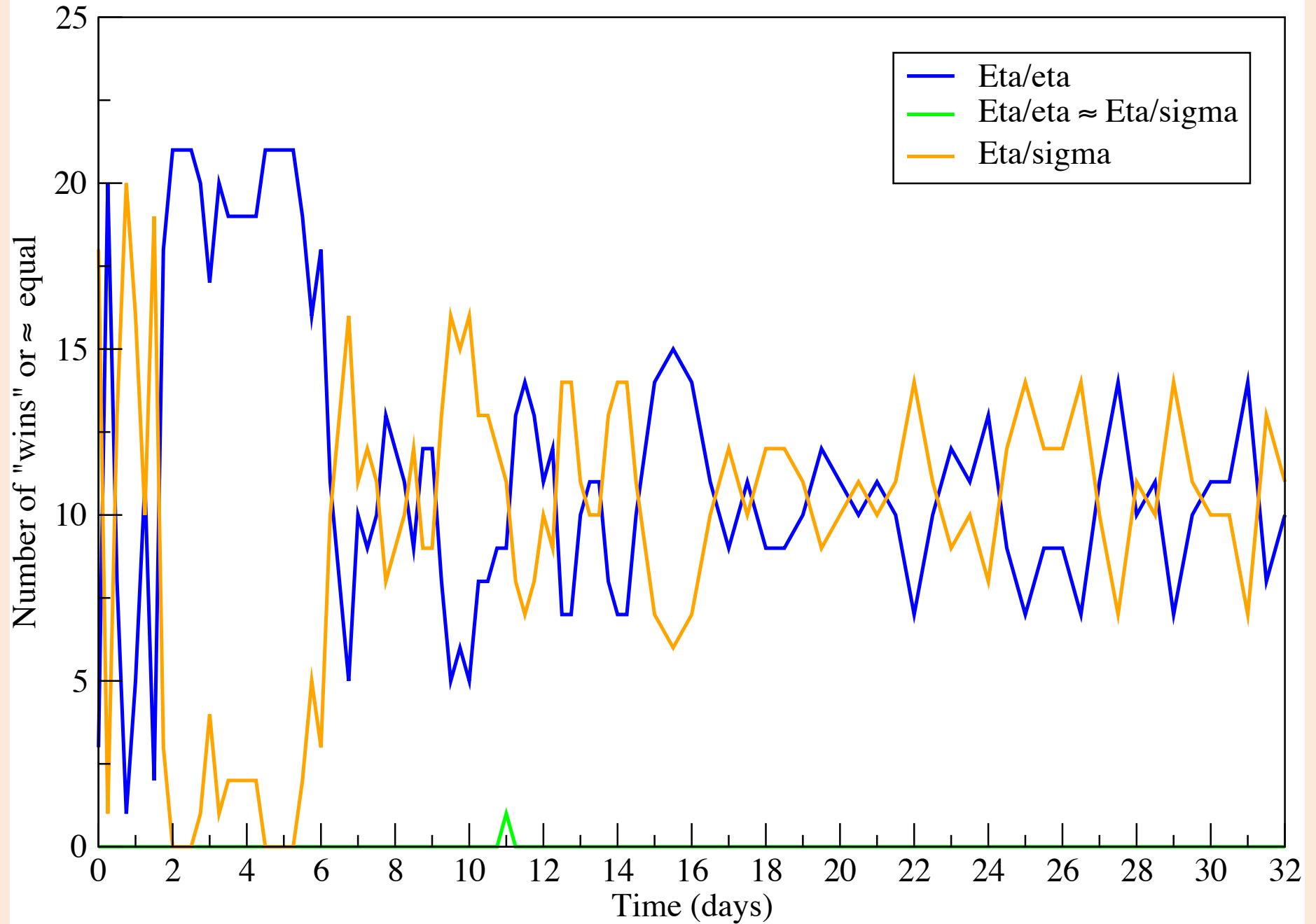
Eta vs.
Eta/
sigma:



Based on RMS difference



Based on SEDS



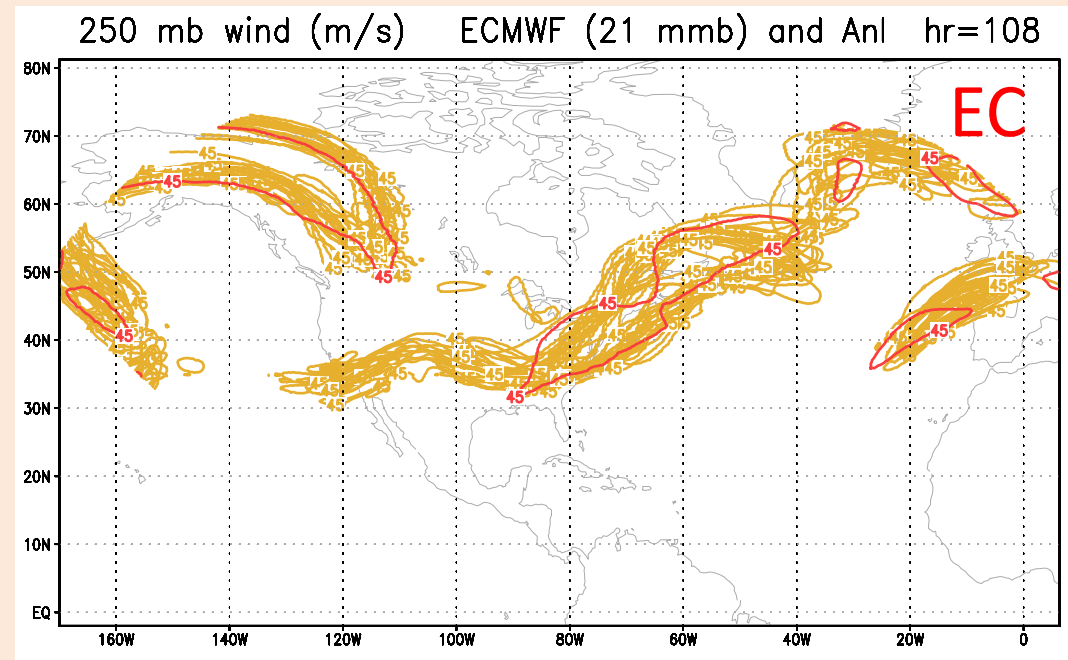
Now:

Contours of all 21
members of areas
of wind speeds
> 45 m/s

Now:

Contours of all 21 members of areas of wind speeds > 45 m/s

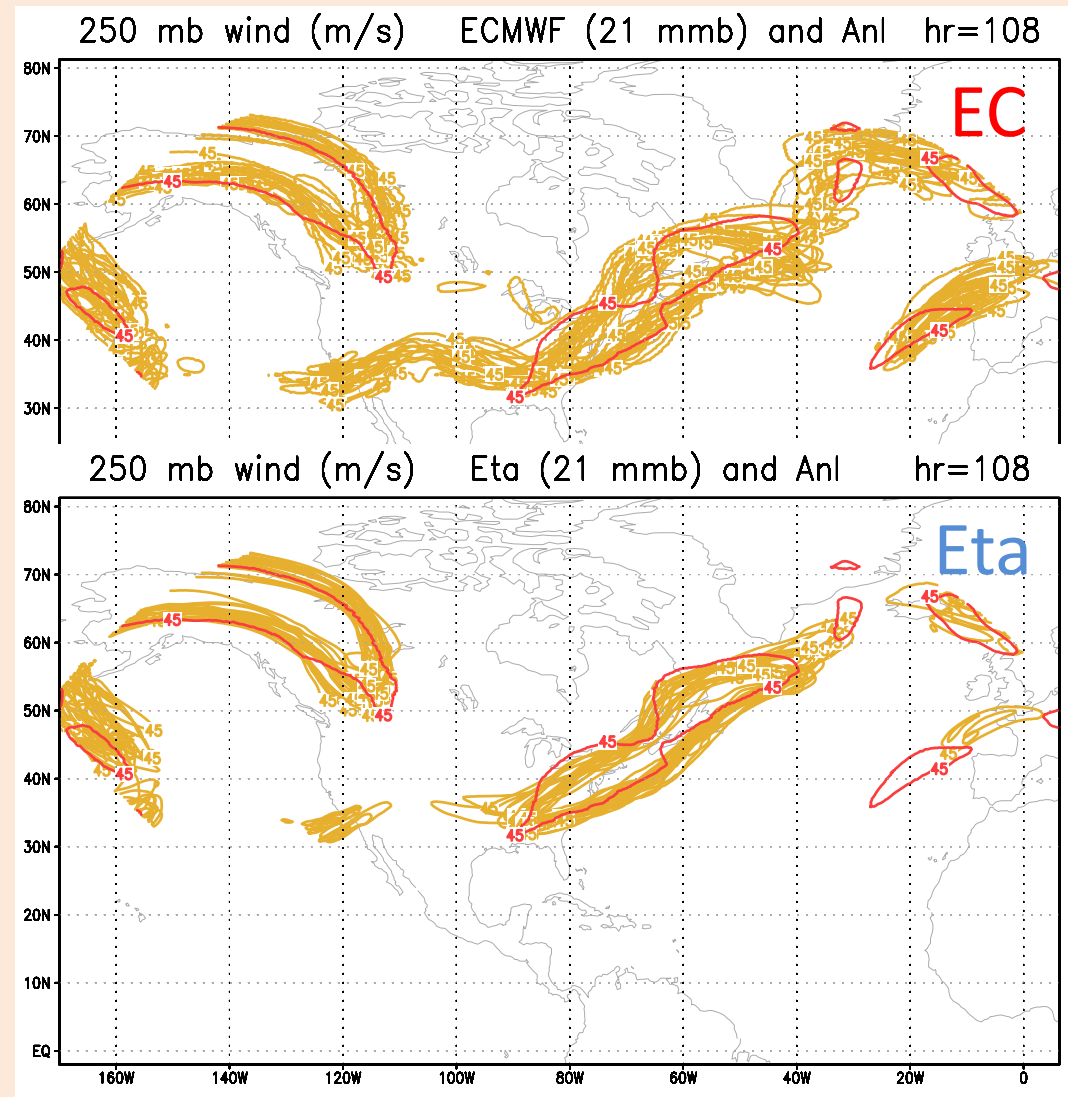
In red are contours of ECMWF verification analysis



Now:

Contours of all 21 members of areas of wind speeds > 45 m/s

In red are contours of ECMWF verification analysis

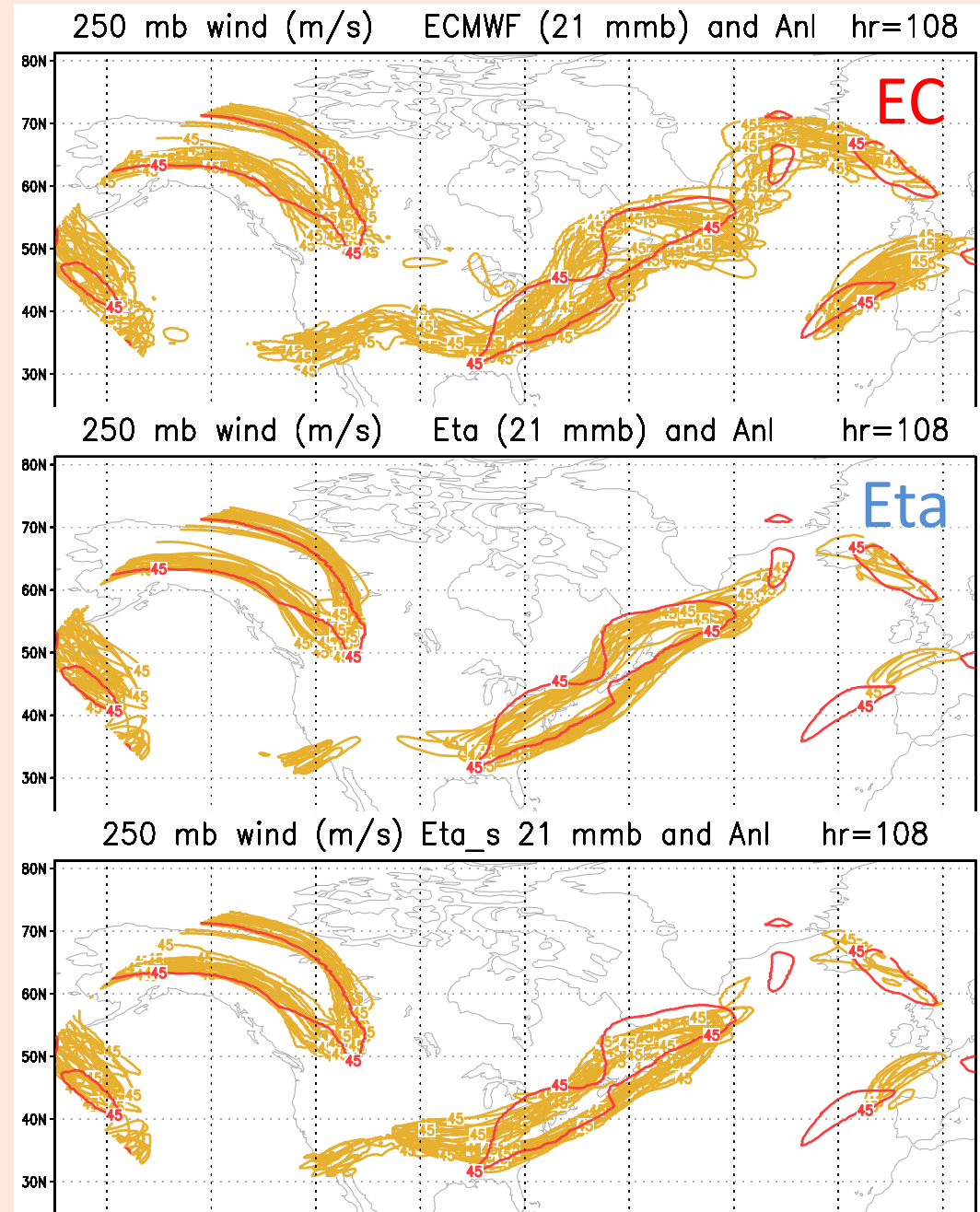


Now:

Contours of all 21 members of areas of wind speeds > 45 m/s

In red are contours of ECMWF verification analysis

Eta/sigma :



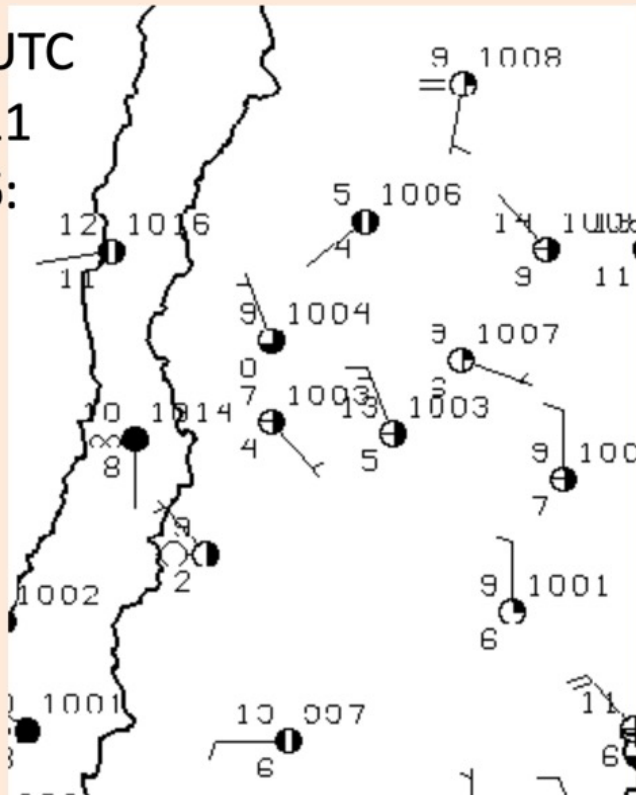
Conclusion 1

- Strong evidence that coordinate systems intersecting topography are able to perform significantly better than terrain-following systems; (in agreement with Steppeler et al. 2013)

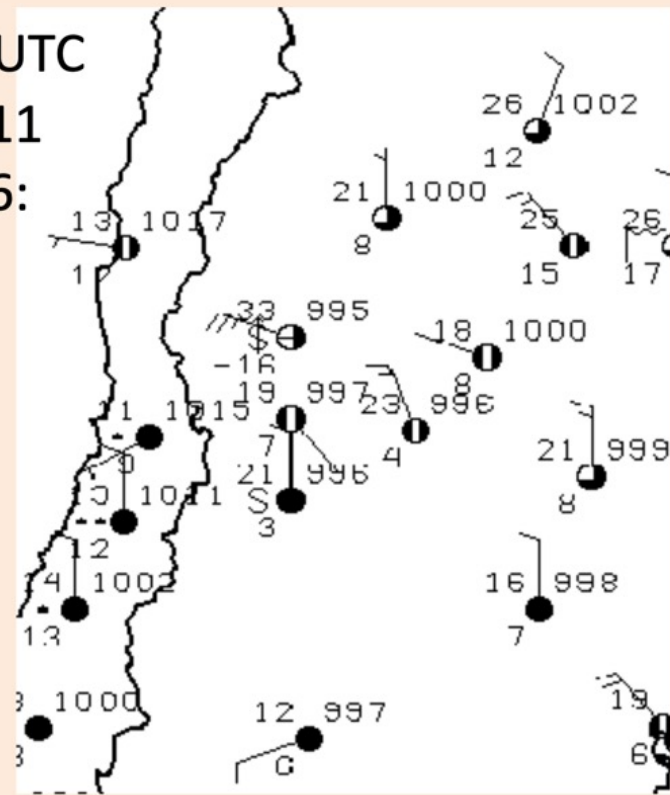
But there must be **more reasons** / why is the Eta/sigma more accurate than the EC ?

Look at the results of a zonda windstorm case:

1200 UTC
July 11
2006:



1800 UTC
July 11
2006:



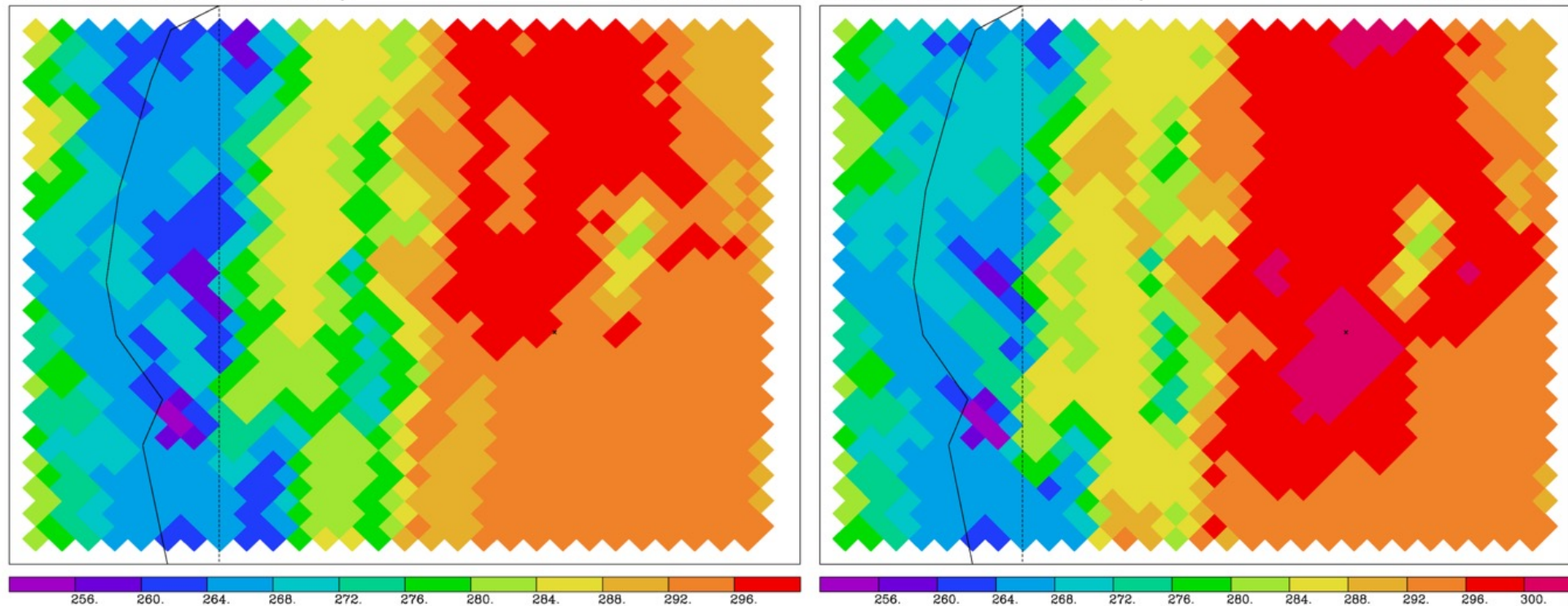
Sections of surface maps illustrating a case of an intense “zonda” windstorm in the lee of the Andes. **Warming from 9 to 33°C in 6 h, 24°C**, is seen at the station San Juan, 630 m above sea level, close to the middle of the above sections. Valid times are displayed in the top left corner of the maps.

VALID 11 Jul 2006 21Z Tuesday

20060710 12UTC 33h fest

VALID 11 Jul 2006 21Z Tuesday

20060710 12UTC 33h fest



Forecast **lowest cell temperatures at 33 h** of the case discussed in Section 9 of Mesinger et al. (2012). The **left-hand** plot shows the result obtained **using (3) for both the slantwise and the vertical advection**, while the **right-hand** plot shows the result with these advectons replaced by **finite-volume schemes**. The roughly vertical line on the left sides of the plots is the Chile-Argentina border, while the straight line is the 70°W meridian. The small cross to the right of the centers of plots shows the place of the San Juan station. **Warming obtained in 9 h is $> 20^{\circ}\text{C}$!**

Conclusion 2:

Finite-volume vertical advection !

Other candidate reasons:

- Arakawa horizontal advection scheme (Janjić 1984);
- Very careful construction of model topography (MV2017), with grid cell values selected between their mean and silhouette values, depending on surrounding values, and no smoothing;
- Exact conservation of energy in space differencing in transformation between the kinetic and potential energy;
-

Thank you!